

# **Role of PINCH during early *Xenopus* embryogenesis**

by

Bhanu Pilli

A thesis  
presented to the University of Waterloo  
in fulfillment of the  
thesis requirement for the degree of  
Master of Science  
in  
Biology

Waterloo, Ontario, Canada, 2012

© Bhanu Pilli 2012

## **Declaration**

I hereby declare that I am the sole author of this thesis. This is a true copy of the thesis, including any required final revisions, as accepted by my examiners.

I understand that my thesis may be made electronically available to the public.

## Abstract

In the *Xenopus* embryo, cell rearrangements during early development require the dynamic modulation of adhesion. Cells primarily use the integrin family of transmembrane receptors for attachment to and interpretation of the extracellular environment. While acting as adhesion receptors, integrins also have bidirectional signalling properties essential for driving cellular movements. The regulation of integrin activity is thought to stem from cytoplasmic assemblies of constitutively expressed molecules. PINCH (Particularly Interesting New cysteine-histidine rich protein), an adapter protein, is part of an IPP complex that has emerged as a key signalling scaffold indispensable for integrin function *in vitro*. As such, I tested the hypothesis that PINCH regulates integrin function in the *Xenopus* embryo.

*Xenopus* PINCH was successfully cloned using RT-PCR. The predicted amino acid sequence of PINCH shares a 98% similarity with mammalian orthologs, and comprises of five highly conserved LIM domains. PINCH mRNA and protein are ubiquitously expressed throughout embryogenesis. In situ hybridization indicates that PINCH mRNA is expressed in the blastocoel roof and the pre-involution mesoderm. The localization and temporal expression of PINCH suggests a role in mediating cell adhesive events during gastrulation.

A functional approach was used to examine the role of PINCH during gastrulation. I used site-directed mutagenesis to generate non-functional LIM1 (LIM1<sub>mut</sub>) and LIM4 (LIM4<sub>mut</sub>) domains that have been proposed to bind ILK and Grb4 respectively. Over-expression of PINCH leads to a delay in blastopore closures, while the expression of both LIM1<sub>mut</sub> and LIM4<sub>mut</sub> relieve this inhibition at lower concentrations. Further analysis indicates that PINCH, LIM1<sub>mut</sub>, and LIM4<sub>mut</sub> inhibit FN matrix assembly independent of integrin adhesion. Contradictory to *in vitro* studies, co-immunoprecipitation analysis indicates that endogenous PINCH does not bind ILK, confirming an integrin-independent role during gastrulation. Furthermore, in the embryo PINCH is found at cell boundaries but does not appear to directly modulate cadherin adhesion. As such this thesis provides evidence that PINCH regulates cell intercalation movements independent of integrin and cadherin receptors and raises the possibility that the LIM4 domain is involved in PINCH regulation of cell adhesion during early development.

## Acknowledgements

I am grateful to Dr. Mungo Marsden (Mungo) for the opportunities he has provided me. I appreciate his guidance, patience, and persistence in bringing the best out of me. I thank him for his mentorship in the lab and in life. He inspired me to overcome my fears, pursue my dreams, and to live a life without regrets. His support and encouragement through the highs and lows helped me get to where I am today. I am also thankful to my committee, Dr. Heidi Engelhardt and Dr. John Heikkila, for their insight and input into my project.

I thank the past and present members of the Marsden lab for the laughs and memories. A special thanks to Catherine Studholme for her friendship, patience, and support during my time here. I will miss the lab stories and every day shenanigans that made those long days and nights in the lab feel a little shorter.

Special thanks to Catherine Skrypka for her endless support and encouragement. Her perspective always kept me grounded and her ability to inspire confidence in me helped me overcome a lot of adversity. Thanks to Jagdeep Singh Jassi for his support, encouragement, and for always believing in my abilities and pulling me through the finish line.

Life is short; Live it to the fullest! My late friend Andrea taught me this the hard way. Thank you for laughs, tears, and cherishable memories which I will forever remember. Special thanks to Hillary Kantorovich for inspiring me to dream big, pushing me past my physical limits, and helping me conquer each day and move one step closer to my fitness goals. Thanks to Deb Hudspeth for sticking with me through the highs and lows and for helping me stay away from those bad carbs. Thanks to Matt Wyatt and Brendan Smith for the constant motivation and gym rants. A special thanks to Tyler Sarry for his continued inspiration and support and to my fitness family for showing me that hard work and determination are key ingredients to become a success story...

My boundless gratitude goes out to my brother, Deepak, for always being there for me. Thanks to my mother, Sudevi, for her patience, support and encouragement, and my father, Narasimham, for supporting my studies now and always. Thank you for having the confidence in me for not following in someone's footsteps but to pave my own path along the way.

# Table of Contents

Declaration.....	ii
Abstract.....	iii
Acknowledgements .....	iv
Table of Contents.....	v
List of Figures.....	vii
List of Tables .....	ix
List of Abbreviations .....	x
Chapter 1 . Introduction	
1.1 Integrin signalling during <i>Xenopus</i> gastrulation.....	1
1.2 Regulation of Cell Adhesion .....	6
1.3 Particularly Interesting New Cysteine Histidine-rich protein (PINCH) .....	7
1.4 Experimental Objectives.....	10
Chapter 2 . Materials and Methods	
2.1 Plasmid Constructs and generation of <i>in vitro</i> transcripts .....	11
2.2 Embryo Culture and Manipulations.....	12
2.3 Cell Culture and Transfections .....	13
2.4 Reverse Transcription-Polymerase Chain Reaction (RT-PCR).....	14
2.5 RNA in situ hybridization (ISH).....	14
2.6 Western Blot Analysis .....	15
2.7 Co-Immunoprecipitation.....	16
2.8 Animal cap experiments .....	16
2.9 Fibronectin Assays .....	17
2.10 Immunofluorescence and Microscopy.....	18
Chapter 3 . Experimental Results	
3.1 Cloning <i>Xenopus</i> PINCH.....	21
3.2 Temporal and Spatial Expression of PINCH.....	25
3.3 PINCH and <i>Xenopus</i> gastrulation.....	31
3.3.1 Characterization of PINCH mutation constructs .....	31
3.3.2 Examining a role for PINCH in <i>Xenopus</i> gastrulation.....	31
3.4 PINCH and FN matrix assembly .....	39

3.4.1 PINCH over-expression inhibits FN matrix assembly.....	39
3.4.2 PINCH and Integrin Adhesion.....	41
3.4.3 PINCH and Cadherin Adhesion.....	48
Chapter 4 . Discussion	
4.1 Cloning and Characterization of <i>Xenopus</i> PINCH .....	54
4.2 PINCH is required for <i>Xenopus</i> embryogenesis .....	56
4.3 PINCH and Cell Adhesion.....	57
4.3.1 Effect of PINCH on Cell-Matrix Adhesion .....	57
4.4. Conclusions .....	61
Chapter 5 . Future Directions.....	63
References .....	65
Appendix A.....	72

## List of Figures

Figure 1	Known vertebrate $\alpha$ and $\beta$ subunits	p. 2
Figure 2	FN matrix assembly <i>in vivo</i> requires cell-cell and cell-matrix adhesion	p. 3
Figure 3	Radial cell intercalation and mediolateral cell intercalation in the embryo and explanted tissues	p. 5
Figure 4	Members of the ILK-PINCH-Parvin (IPP) complex	p. 7
Figure 5	<i>Xenopus laevis</i> PINCH (PINCH)	p. 23
Figure 6	Amino acid sequence alignment of <i>Xenopus</i> PINCH and known PINCH orthologs	p. 24
Figure 7	Comparison of <i>Xenopus</i> PINCH with known PINCH homologs	p. 25
Figure 8	PINCH mRNA is constitutively expressed throughout early <i>Xenopus</i> embryogenesis	p. 28
Figure 9	Spatial Expression of PINCH mRNA during early embryogenesis	p. 29
Figure 10	Spatial Expression of PINCH mRNA during gastrulation	p. 30
Figure 11	PINCH protein is constitutively expressed during early embryogenesis	p. 31
Figure 12	GFP-tagged PINCH constructs localize to focal adhesions in <i>Xenopus</i> A6 kidney cells	p. 35
Figure 13	Over-expression of PINCH delays blastopore closures	p. 36
Figure 14	Protein expression in embryos microinjected with PINCH mRNA	p. 37
Figure 15	PINCH over-expression does not affect mesodermal patterning.	p. 38

Figure 16	PINCH controls epiboly in the BCR	p. 39
Figure 17	PINCH is required for FN matrix assembly	p. 41
Figure 18	Quantification of activin-treated cell adhesion to FN substrates	p. 45
Figure 19	PINCH does not affect activin-induced cell migration	p. 46
Figure 20	PINCH is not permissive for convergent extension	p. 47
Figure 21	PINCH is unlikely to interact with ILK <i>in vivo</i>	p. 48
Figure 22	GFP-tagged PINCH constructs localize to cell-cell contact sites in activin-induced animal cap cells	p. 51
Figure 23	PINCH localizes to adherens junctions at cell-cell boundaries in the BCR	p. 52
Figure 24	PINCH colocalizes with $\beta$ -catenin at cell-cell boundaries in the BCR	p. 53
Figure 25	PINCH does not influence cell adhesion to C-Cadherin	p. 54



## List of Tables

Table 1	Primer Sequences	p. 11
Table 2	Antibodies	p. 19

## List of Abbreviations

BCR	Blastocoel Roof
BSA	Bovine Serum Albumin
CE	Convergent extension
CH	Calponin homology
CHO	Chinese Hamster Ovary
Co-IP	Co-immunoprecipitation
ECM	Extracellular Matrix
Eph	Erythropoietin-producing human hepatocellular carcinoma
ESB	Embryo solubilization buffer
FA	Focal Adhesion
F-actin	Filamentous actin
FBS	Fetal Bovine Serum
FN	Fibronectin
GFP	Green Fluorescent Protein
Grb4	Growth receptor bound protein-4
HCG	Human Chorionic Gonadotropin
HRP	Horse Radish Peroxidase
IEC	Intestinal epithelial cells
ILK	Integrin-linked Kinase
IPP	ILK-PINCH-Parvin Complex
ISH	In Situ Hybridization
LIM	Lin-11, Isl-1, Mec-3
MBS	Modified Barth's Saline
MBT	Mid-blastula transition
MIB	Mediolateral cell Intercalation behaviour
MSC	Mesenchymal Stem Cells
MSS	Modified Stearn's Solution
NES	Nuclear Export Signal
NI	Non-injected
NLS	Nuclear localization Signal
PAK	p21-activated Kinase
PBS	Phosphate Buffer Saline
PDGF	Platelet-derived Growth Factor
PH	Pleckstrin homology
PINCH	Particularly Interesting New Cysteine Histidine-rich protein
PMSF	Phenylmethylsulfonyl Fluoride
Rsu-1	Ras Suppressor Protein-1
RT	Room temperature

RT-PCR	Reverse-Transcriptase Polymerase Chain Reaction
SDS-PAGE	Sodium Dodecyl Sulfate Polyacrylamide Gel Electrophoresis
TBS	Tris Buffer Saline
T $\beta$ -4	Thymosin beta-4
TCA	Trichloroacetic Acid
TGF	Transforming Growth Factor
WT1	Wilms tumour gene 1

# Chapter 1. Introduction

## 1.1 Integrin signalling during *Xenopus* gastrulation

The regulation of adhesive contacts between cells and the extracellular matrix (ECM) underlies many morphogenetic processes during early development. The dynamic regulation of cell-ECM adhesion is primarily mediated through the integrin family of adhesion receptors. Integrins consist of non-covalently linked trans-membrane  $\alpha$  and  $\beta$  subunits. These heterodimeric receptors are capable of propagating biochemical signals bi-directionally across the cell membrane. As such cells use integrin receptors to interpret their immediate microenvironment and determine cellular behaviour.

Integrins are a diverse family of receptors that mediate the adhesive property of cells. In mammals, there are at least 18 $\alpha$  and 8 $\beta$  subunits that combine to form 24 known integrin heterodimers (Figure 1, reviewed by (1)). There is a reduced diversity of integrin subunits in invertebrates. For instance, *Caenorhabditis elegans* has two  $\alpha$  subunits ( $\alpha$ PAT-1 and  $\alpha$ PAT-2) and one  $\beta$  subunit ( $\beta$ PAT-3) while *Drosophila melanogaster* has five  $\alpha$  subunits ( $\alpha$ PS1-5) and two  $\beta$ -subunits ( $\beta$ PS and  $\beta$ v) (2). Both  $\beta$ PAT-3 and  $\beta$ PS are closely related to vertebrate  $\beta$ 1 subunits suggesting that these orthologs represent a primordial receptor. Only a select group of subunits exists in *Xenopus laevis* (Figure 1; labelled in red). Three integrins  $\alpha$ 5 $\beta$ 1 (3),  $\alpha$ V $\beta$ ? (4), and  $\alpha$ 3 $\beta$ 1 (5) are expressed during gastrulation; however, the  $\alpha$ 5 $\beta$ 1 integrin is the only functional receptor (6).

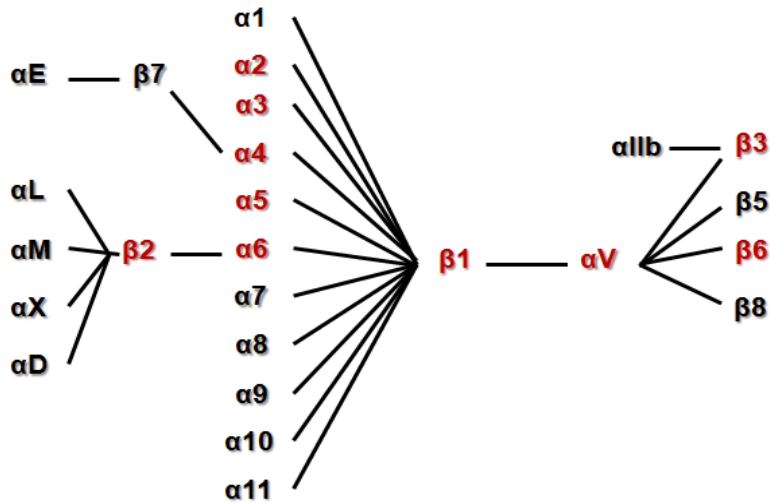


**Figure 1: Known vertebrate  $\alpha$  and  $\beta$  integrin subunits.** The spider diagram displays the known  $\alpha\beta$  subunit combinations in vertebrates (adapted from Hemler et al., 1992 (7)). Eighteen  $\alpha$  subunits and eight  $\beta$  subunits are able to generate 24 different integrins. Integrins highlighted in red indicate the functional integrin subunits in *Xenopus laevis*.

During early *Xenopus* development, the  $\alpha5\beta1$  integrin is ubiquitously expressed in the embryo. A maternal pool of both  $\beta1$  and its associated  $\alpha5$  subunit are present as precursors in the egg prior to fertilization (8). Upon fertilization  $\alpha5\beta1$  integrin localizes to the newly formed plasma membranes during cleavage. (9). In the blastula all cells express  $\alpha5\beta1$  integrin and secrete soluble fibronectin (FN) (10). However, FN fibrillogenesis occurs only on the free surface of blastocoel roof (BCR) at the start of gastrulation, indicating that the adhesive properties of the  $\alpha5\beta1$  receptor are modified in a spatially restricted manner. The current model for FN fibrillogenesis suggests a multistep integrin-dependent process (11-13) (Figure 2). Initially, BCR cells use  $\alpha5\beta1$  integrin to bind FN at cell-cell boundaries. There is an increase in cell-cell adhesion due to an increase in cadherin surface expression. A change in cortical actin polymerization and myosin-light chain II phosphorylation generate tension along the BCR which allow the FN-bound integrin receptors translocate centripetally along the cell surface. The

increased tension across the BCR is then transmitted to FN through  $\alpha5\beta1$  integrin. Subsequent unfolding of FN dimers exposes a self-assembly motif that promotes FN-FN interactions and initiates the assembly of a matrix (14).

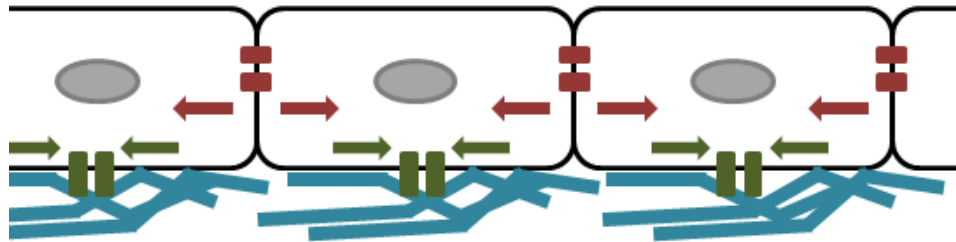


**Figure 2: FN matrix assembly *in vivo* requires cell-cell and cell-matrix adhesion.** At the onset of gastrulation, BCR cells use  $\alpha5\beta1$  integrin (green rectangles) to bind to FN. An increase in cell-cell cohesion (red rectangles) increases the mechanical tension in the BCR (red arrows). Upon a change in tissue tension, integrin-FN complexes move centripetally from cell-cell boundaries (green arrows). Subsequent unfolding of FN promotes FN-FN interactions and initiates the assembly of a FN matrix (blue lines) (adapted from Weber et al (2011) (15)).

The regulation of integrin adhesive properties during early gastrulation can be modulated through signals emanating from inside the cell (inside-out signalling). Such signalling events have been characterized using *ex vivo* assays. Cells isolated from the animal cap region of a blastula have the ability to attach to FN using the Arg-Gly-Asp (RGD) sequence in the central cell binding domain (CCBD) (16). After activin exposure, these cells acquire the ability to bind to the synergy domain and to spread and migrate on FN (16). As there is no change in integrin expression during this change in cell behaviour, these experiments suggest inside-out signalling mechanisms influence a change in integrin adhesive properties during early gastrulation events such as mesoderm involution and migration (16).

As gastrulation proceeds, FN matrix defines tissue domains undergoing large-scale rearrangements in the embryo. At these tissue boundaries  $\alpha 5\beta 1$  integrin transmits signals from FN into the cell to drive cell intercalation behaviour. Radial intercalation in the deep cells of the animal cap drives the process of epiboly, the spreading and thinning of the superficial ectoderm (Fig. 3A) (17). While epiboly is primarily localized in the animal portion and marginal zone of the BCR, cell intercalation also drives tissue rearrangements in the marginal zone of the embryo (17). The pre-involution mesoderm cells intercalate initially in the radial direction, and then in the medial-lateral direction to drive involution. The post-involution mesoderm then extends anterior through further medial-lateral intercalations resulting in the convergence and extension of the tissue (Figure 3B) (17). Interfering with  $\alpha 5\beta 1$ -FN ligation results in loss of the typical polarized arrangement of cell protrusions observed in intercalating tissues (46). These observations suggest that both inside-out and outside-in signalling through  $\alpha 5\beta 1$  is required for both the assembly of a FN matrix and for driving FN-mediated cell rearrangements during gastrulation.

While the cell rearrangements occurring during *Xenopus* development are well characterized the molecular basis of integrin-mediated changes in cell behaviour are not well known. However, the molecules and signalling pathways regulating integrin function have been extensively studied in mammalian cell culture and to a certain extent these studies can be extrapolated to *Xenopus* gastrulation.

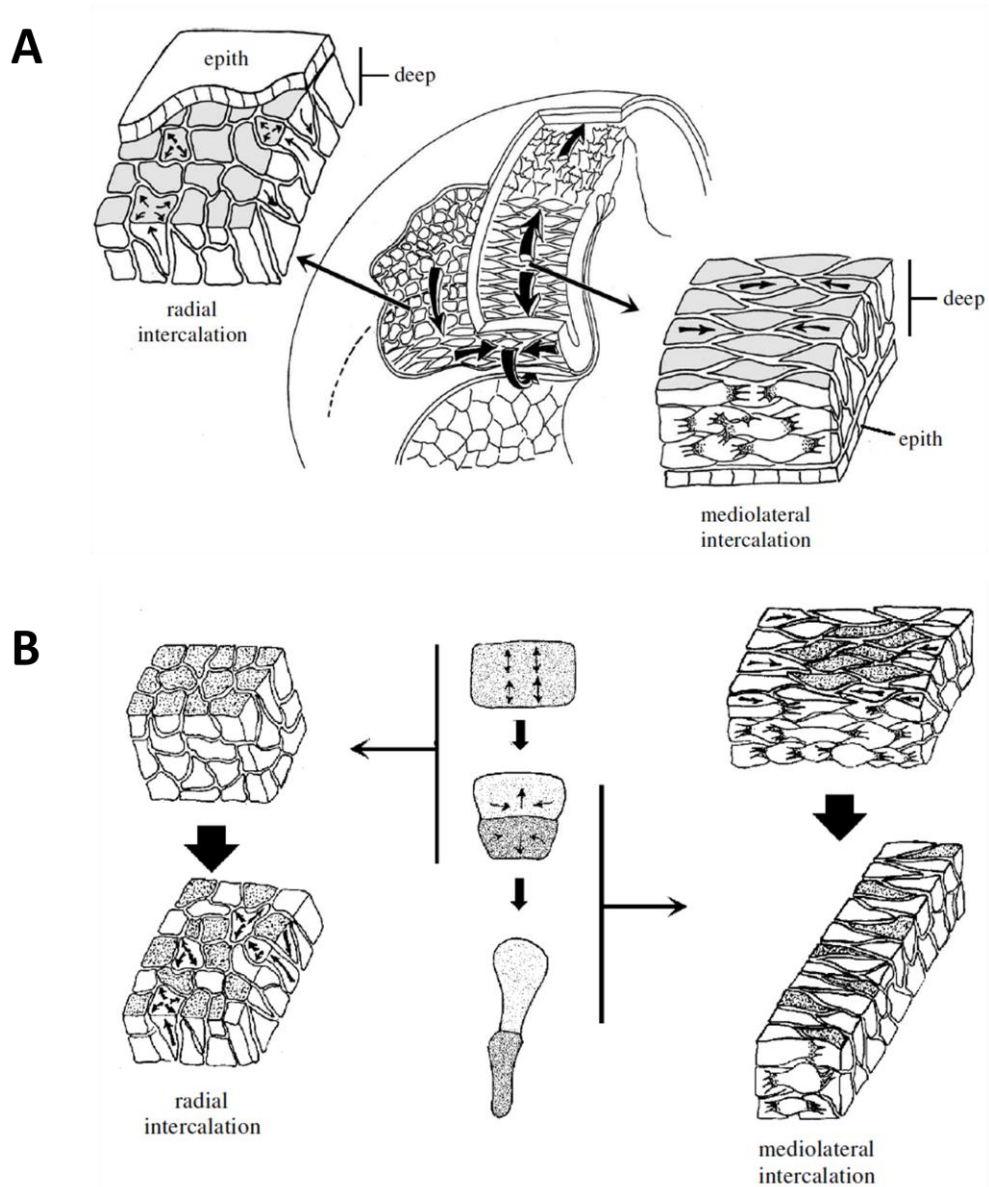


**Figure 3: Radial and medial-lateral cell intercalation in the embryo and explanted tissues.** Epiboly is driven by radial intercalation of multiple layers of deep cells along the BCR of the embryo while the superficial epithelium spreads to cover the whole embryo (A, left panel). In the marginal zone, CE occurs first by radial intercalation followed by medial-lateral intercalation in presumptive mesodermal tissue (A, right panel). In explants, radial intercalation occurs when several deep cells intercalate to produce fewer layers (B, left panel). During medial-lateral intercalation, deep cells intercalate in the medial lateral direction to produce a longer, narrower tissue (B, right panel). Adapted from (17)



## 1.2 Regulation of Cell Adhesion

Integrins are trans-membrane receptors that not only provide a physical linkage between the ECM and the cytoskeleton but also initiate or modify intracellular signalling pathways that can mediate changes in cell behaviour. Initial integrin ligation to the ECM promotes clustering of integrins and the formation of localized cytoplasmic protein assemblies that are collectively known as focal adhesions (18). Focal adhesions are dynamic structures and over 150 different cytoplasmic molecules are known to be associated with focal adhesions (19). These signalling assemblies are organized through multi-domain adaptor proteins that are themselves regulated by the recruitment of kinases and phosphatases. While the composition of focal adhesions is diverse and cell type specific my focus is on PINCH, a member of the Integrin-linked Kinase-PINCH-Parvin (IPP) complex (Figure 4). The IPP complex is formed in the cytosol and recruited to integrins following ligation to the ECM (20). Integrin-linked Kinase (ILK) is the central member of the complex and binds directly to  $\beta 1$  and  $\beta 3$  integrin cytoplasmic tails (21). The parvins link ILK to the actin cytoskeleton, while PINCH is thought to link ILK to signalling pathways initiated through growth factor receptor ligation.

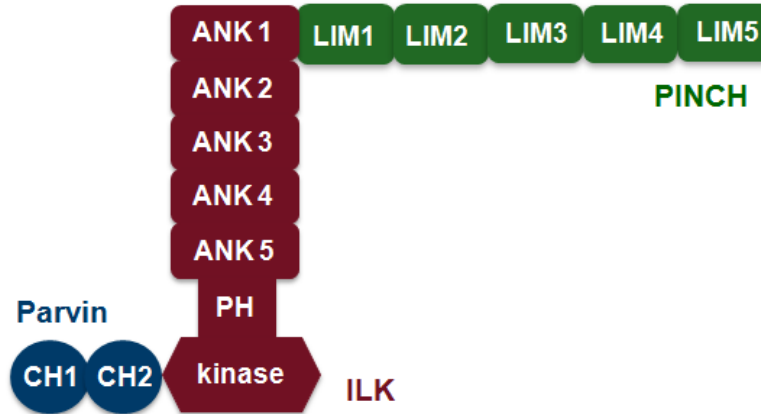


**Figure 4: Members of the ILK-PINCH-Parvin (IPP) complex.** Integrin-linked Kinase (ILK) consists of a central pleckstrin homology (PH) domain, an ankyrin repeat (ANK) domain at the amino terminus that binds to Particularly Interesting New Cysteine Histidine-rich protein (PINCH), and a kinase domain at the carboxy terminus that binds to  $\beta$ -parvin. PINCH consists of five LIM [Lin11, Isl-1, Mec-3] domains and parvin has two calponin homology (CH) domains CH1 and CH2 (adapted from (20)).

### 1.3 Particularly Interesting New Cysteine Histidine-rich protein (PINCH)

PINCH is a 35.8 kDa protein first discovered as a marker for senescent red blood cells in the human fetal liver (22). Since its discovery in 1994, PINCH has been shown to participate in the fundamental cell adhesion processes regulating cell proliferation and survival, and alterations in PINCH expression is associated with several cancers as well as neuronal damage. Cell adhesion integrin receptors have been well established to regulate cell migration, invasion, proliferation, and survival during the progressive stages of cancer. The expression levels of integrin-associated proteins such as PINCH have been correlated with the different stages of metastasis. For instance, clinical studies revealed PINCH is over-expressed in the stroma of human cancers including breast, prostate, lung, and colon cancers and has been established as an independent prognostic indicator of colorectal cancer (23-26). Further analysis showed more abundant

expression of PINCH in the stromal cells at the invasive margin than the inner tumor area (23, 27), suggesting a possible role in tumor progression and development. Recent studies have reported increased PINCH expression in post-injury Schwann cells and dorsal root ganglia neurons, suggesting a role in both neuronal damage and myelin loss (28). Together, these clinical studies emphasize the importance in studying the cellular functions of PINCH and its role in regulating cell adhesion molecules such as integrin receptors.

PINCH is a member of the LIM (Lin-11, Isl-1, Mec-3) family of proteins. PINCH is comprised of five LIM domains and thus the ability of these domains to bind specific proteins is thought to regulate its cellular function and localization. The LIM1 domain of PINCH is known to mediate binding with ILK and this interaction is required for the formation and stability of the IPP complex (21). Disrupting the PINCH-ILK interaction in Chinese hamster ovary (CHO) cells abolished the localization of ILK to integrin-rich focal adhesions (29). As such PINCH has been postulated to play a role in ILK localization and function in cells. Over-expression of ILK in rat intestinal epithelial cells (IEC-18) increased cell-surface binding to FN (30). An increase in ILK localization to focal adhesions enhances spreading in CCL39 cells plated on FN (31). Together, these observations suggest that the PINCH-ILK interaction may play a role in regulating integrin adhesion to FN.

The LIM4 domain of PINCH mediates binding with the adapter protein Grb4 (Growth factor receptor-bound protein-4) (32). There is evidence that the cross-talk between growth factor receptors and integrin receptors is required for modulating cell behaviour. In human mesenchymal stem cells (MSCs), cell adhesion to FN induces co-localization of Platelet-derived growth factor receptor- $\beta$  (PDGFR- $\beta$ ) and  $\alpha 5\beta 1$  integrin receptors. Disrupting the ligand binding of either receptor significantly reduces MSC migration on FN (33). Cytoplasmic molecules that

associate with both integrin and growth factor receptors are candidates to regulate such cross-talk. It is likely that Grb4 plays a key role in this cross-talk as Grb4 is recruited to focal adhesions and has been shown to bind growth factor receptors (34, 35). Such a role for Grb4 is supported by experiments in mouse embryo fibroblasts where knockdown of Grb4 severely reduced the number of focal adhesions and impaired PDGF-induced chemotaxis (32).

PINCH also contains a short C-terminal region that contains a leucine-rich nuclear export signal (NES) and nuclear localization signal (NLS) (36). As such PINCH has been proposed to act as a shuttling protein between the cytoplasm and the nucleus. Recent evidence in mammalian cell culture supports this hypothesis as PINCH has been found to physically interact with a key nuclear transcription factor WT1 in human podocytes (37). WT1 is a product of Wilms tumour gene 1 and is expressed during early embryonic kidney development and plays a crucial role in mammalian nephron formation (37).

While PINCH has been predominantly examined in tissue culture models there are limited studies in invertebrate model systems. In *Caenorhabditis elegans* the PINCH ortholog UNC-97 has been shown to colocalize with ILK and integrin at sites of muscle cell attachment (38). Similarly, genetic and loss-of-function studies in *Drosophila melanogaster* demonstrate that PINCH is essential for dorsal closure and is found with ILK at muscle-attachment sites (39). However, the recruitment of ILK and PINCH were not directly correlated suggesting that the roles described for molecules that act downstream of integrin ligation in tissue culture are not always directly transferrable to *in vivo* model systems. While *C. elegans* and *Drosophila* have provided some information on PINCH function (40, 41) they are not established models for investigating cell adhesion events. *Xenopus* has proven to be a strong model organism to investigate integrin function. The morphogenetic movements during early embryogenesis

behind  $\alpha 5\beta 1$ -FN ligation have been well characterized (42-47). The presence of only one active integrin receptor,  $\alpha 5\beta 1$ , and a single ligand FN during gastrulation makes it a simple yet powerful model to examine molecular mechanisms regulating integrin function.

#### **1.4 Experimental Objectives**

The goal of this study is to characterize *Xenopus* PINCH and determine the role of this protein in the *Xenopus* embryo. The first objective of this study was to clone *Xenopus* PINCH and determine the temporal and spatial expression during development using RT-PCR, western blotting, and in situ hybridization. My next aim was to determine the endogenous role of PINCH in the *Xenopus* gastrula. PINCH is a multiple LIM domain adaptor protein known to participate in several signalling pathways. As such I predicted that mutations of the LIM domains would reveal a role for PINCH during gastrulation. Mutations in the LIM1 (LIM1<sub>mut</sub>) and LIM4 (LIM4<sub>mut</sub>) domains were created by site directed mutagenesis and tested both in vitro and in vivo. The third objective of this study was to determine if PINCH regulates cell adhesion. I used ex-vivo assays to estimate the role PINCH plays in both cell-ECM as well as cell-cell adhesion.

## Chapter 2. Materials and Methods

### 2.1 Plasmid Constructs and generation of *in vitro* transcripts

Primers were designed for Reverse-Transcriptase Polymerase Chain reaction (RT-PCR; primers listed in Table 2.1) to isolate the coding region of a known *Xenopus laevis* PINCH expressed sequence tag (Genbank Accession # NM01091652). The resulting PCR product was digested using *BamHI* and *XbaI* restriction enzymes and ligated into the *BamHI* and *XbaI* sites of Bluescript SK II (+) to generate the PINCH-BS construct. The insert was confirmed to be the *Xenopus laevis* ortholog of PINCH by sequencing.

Site-directed mutagenesis was used to alter the amino acid 40 in the LIM1 domain from AQCF to AACF to generate the LIM1<sub>mut</sub> construct. Similarly, amino acids 208 and 209 in the LIM4 domain were altered from CRRP to CAAP to generate the LIM4<sub>mut</sub> construct. Both inserts were confirmed by sequencing. The primers used to generate the constructs are listed in Table 2.1

For *in vivo* imaging PINCH was tagged with GFP at the N terminus. PINCH, LIM1<sub>mut</sub>, and LIM4<sub>mut</sub> were amplified by PCR using *Pfu Polymerase* (primers listed in Table 2.1). The PCR products were digested using *BamHI* and *XbaI* and ligated into the *BamHI* and *XbaI* sites of pCS2 GFP-N1 (Gift from J Miller). In frame insertion of constructs was confirmed by sequencing.

**Table 1: Primer Sequences.** Underlined nucleotides correspond to restriction enzyme sites. Bold sequences correspond to nucleotide changes used to generate non-functional LIM1 and LIM4 domains

Clone	Primer DNA Sequence
<b>PINCH-BS</b>	
xpinch forward	5'-CCC <u>GGATCCT</u> CCCCCAATCTCTGGCTCC-3'
xpinch reverse	5'-CCCTCTAG <u>AATGCTT</u> ATCCAAGTCTTCACCCTG-3'
<b>LIM1<sub>mut</sub>-BS</b>	
Lim1 mut forward	5'-GCAGTGTTTTGTATGTGCT <b>GCGT</b> GTTTCAGCAGTTTCC-3'
Lim1 mut reverse	5'-GGAAACTGCTGAAAGCACGCAGCACATACAAAACACTGC-3'
<b>LIM4<sub>mut</sub>-BS</b>	
Lim4 mut forward	5'-GCCTATATGTGGGGCTTGC <b>GCAGC</b> ACCAATTGAAGGACGTGT-3'
Lim4 mut reverse	5'-CGACACGTCCTTCAATTGGTGCTGCGCAAGCCCCACATATAGG-3'
<b>GFP-tagged PINCH, LIM1<sub>mut</sub>, LIM4<sub>mut</sub></b>	
GFP pinch forward	5'-CCC <u>GGATC</u> CCATGCTGGGCGTTGTGGGGATGACG-3'
GFP pinch reverse	5'-CCCTCTAG <u>AATGCTT</u> ATCCAAGTCTTCACCCTG-3'

## 2.2 Embryo Culture and Manipulations

Sexually mature wild-type and albino *Xenopus laevis* frogs were purchased from Nasco (Fort Atkinson, Wisconsin) and housed in the Department of Biology Aquatic facility at the University of Waterloo. Individual female frogs were injected with 800 units of human gonadotropin (hCG) (Chorulon; CDMV, St Hyacinthe, Quebec) and placed at 18-20 °C overnight to induce spawning. Eggs were manually obtained from females and fertilized *in vitro* using standard methods (48). Embryos were staged according to Niewkoop and Faber (49). Prior to injection, embryos were dejellied in 2% cysteine in 0.1 x Modified Barth's Saline (1 x MBS; 88 mM sodium chloride, 1 mM potassium chloride, 0.7 mM magnesium sulphate, 1 mM HEPES, 5 mM sodium bicarbonate, 0.1 mM calcium chloride, pH 7.6) (46).

Dejellied embryos were transferred into 0.5 x MBS with 4% Ficoll 400 (Bioshop Burlington, Ontario) for microinjection. Microinjection needles were pulled using a Narishige PC-10 puller (East Meadow, NY) and a Narishige IM300 pressure injector (East Meadow, NY) was used for microinjections. Two cell embryos were injected in the animal hemisphere with individual mRNAs. The amounts of each construct are described in individual experiments in the results section. Following injection embryos were cultured in 0.1 x MBS.

### **2.3 Cell Culture and Transfections**

*Xenopus* A6 cells (ATCC# CCL-102) were maintained in 66% L-15 media (Sigma, Oakville, ON) supplemented with 10% fetal bovine serum (FBS; Wisent, Montreal, QC), 1% L-glutamine (Wisent, Montreal, QC), 1% sodium pyruvate (Sigma, Oakville, ON), and 1% penicillin/streptomycin solution 100x (Wisent, Montreal, QC). Cells were cultured to 60-80% confluence before being detached using trypsin/EDTA (0.05% trypsin, 0.53 mM EDTA; Wisent, Montreal, Quebec) and plated on 60 mm glass bottom dishes in 66% complete L-15 media.

The growth medium was replaced with 66% L-15 media without serum (incomplete media) prior to transfection. One  $\mu\text{g}$  of purified PINCH, LIM1<sub>mut</sub>, or LIM4<sub>mut</sub> DNA in a 10  $\mu\text{L}$  volume was incubated with 100  $\mu\text{L}$  66% incomplete L-15 media. Five  $\mu\text{L}$  of Lipofectamine reagent (Invitrogen, Burlington, ON) was diluted in 100  $\mu\text{L}$  66% incomplete L-15 in a separate tube. Both solutions were incubated for 15 min at RT. Diluted DNA and Lipofectamine were gently mixed and added to each transfection dish. After a 6 h incubation period, transfection media is replaced with 66% complete L-15 media, cells were cultured overnight and imaged two days post-transfection.



## 2.4 Reverse Transcription-Polymerase Chain Reaction (RT-PCR)

RNA was extracted from frozen embryos using acid guanidium-thiocyanate-phenol-chloroform method (50). Briefly, 25 embryos were lysed in 0.5 mL denaturing solution (4M guanidium thiocyanate, 25 mM sodium citrate pH 7.0, 0.5% sarcosyl lauryl sarcosine, and 100 mM dithiothreitol (DTT)). Embryo lysates were phenol-chloroform extracted and total RNA precipitated with isopropanol. Additional precipitation steps with lithium chloride and sodium acetate were added to increase the purity of the extracted RNA. Concentration and quality of RNA were assessed by measuring the absorbance at 260 and 280 nm using an Ultrospec 2100 pro (GE Health Care, Baie d'Urfe, QC).

RT-PCR was performed using a standard protocol (51). First strand cDNA was prepared from 2 µg of total RNA using RevertAid<sup>TM</sup> H Minus First Strand cDNA synthesis kit (Fermentas, Burlington, Ontario) using random primers in a 20 µL reaction. PCR reactions (50 µl) were carried out using *Taq* DNA polymerase (1.25 units/reaction) and *Taq* buffer (Fermentas, Burlington, Ontario), with 0.2 mM of dNTP's, 1.0 µM of each primer (PINCH forward and reverse primers are listed in Section 2.1) and 2 µL of first strand cDNA. The initial denaturation was carried out at 95°C for 2 min followed by 30 cycles of – denaturation at 95°C for 30 sec, annealing for 60 sec at 55°C, and extension at 72°C for 50 sec. The final extension was carried out for 2 min.

## 2.5 RNA in situ hybridization (ISH)

### *Probe Preparation*

PINCH-BS was digested using *Bam*HI (antisense) or *Xba*I (sense) and linearized using *Not*I.

Digoxigenin –UTP labeled probes were synthesized using 1 ug of linearized plasmid DNA, 10x

transcription buffer (Fermentas, Burlington, Ontario), DIG RNA labeling Mix (Roche, Mississauga, ON) and T3 (sense) or T7 (antisense) polymerase. The transcription reaction was carried out for 2 h at 37°C.

### *In situ hybridization*

Embryos from stages 2, 7, 8, 10.5, 12, 17, and 28 were fixed in 4% formaldehyde in 1x MEMFA (100 mM 3-morpholinopropane-1-sulfonic acid (MOPS), 2 mM ethylene glycol tetraacetic acid (EGTA), 1 mM magnesium sulfate) for 2 h at room temperature. Embryos were hybridized with DIG-labeled PINCH RNA sense and antisense probe following standard protocol (52). Hybridized probe was detected with alkaline phosphatase-coupled anti-DIG antibody (Roche, Mississauga, ON) and visualized using BM purple (Roche, Mississauga, ON).

## **2.6 Western Blot Analysis**

Western blots were performed using standard methods (53). Briefly, embryo lysates were prepared by triturating 5 embryos in 100 µl of cold embryo solubilization buffer (ESB; 100 mM sodium chloride, 1% Triton-X 100, 50 mM Tris (pH 7.5), 1 mM phenyl-methyl sulfonyl fluoride (PMSF), 1 x protease inhibitor cocktail (Roche, Mississauga,ON), 1 mM sodium orthovanadate). Extracts were centrifuged at 4°C for 20 min and supernatant was collected. 20% of 5x sample buffer was added (5x Sample buffer; 312.5 mM Tris (pH 6.8), 25% glycerol, 10% sodium dodecyl sulfate, 50 mM 2-mercaptoethanol, 0.05% bromophenol blue) was added and proteins were fractionated by 12% SDS-PAGE and subsequently transferred to nitrocellulose membranes. The membranes were blocked in 5% nonfat dry milk in TBS, 0.1% Tween-20 over night at 4°C. Primary antibody (listed in Section 2.5.1) incubation was done at room

temperature for 1 h. Primary antibodies were then visualized using either anti-rabbit or anti-mouse horse radish peroxidase (HRP) conjugated antibodies (Jackson Labs, Bar Harbor, ME), and luminal (1.25 mM Luminol; Sigma, Oakville, ON); 0.198mM p-coumaric acid (Sigma, Oakville, ON), 1 M Tris (pH 8.5), 0.03% H<sub>2</sub>O<sub>2</sub>, 30%), on RXB x-ray film (Lab Scientific, Livingston, NJ).

## **2.7 Co-Immunoprecipitation**

Co-immunoprecipitation assays were performed using standard methods (53). Embryo lysates were prepared from stage 11 embryos in embryo solubilization buffer (ESB). Protein G Agarose, fast flow suspension beads (EMD Millipore, Billerica, MA) were pre-washed twice in 1 x PBS and once in 1x ESB. Lysates were pre-cleared with 10 µl pre-washed Protein G beads for 1 hr at 4°C. Protein G beads were removed by centrifugation and lysates incubated with PINCH mouse monoclonal antibody (Abcam, Cambridge, MA) for 1 hr at 4°C. Fifteen µL pre-washed Protein G agarose beads were added for 2 hr at 4°C. Beads were washed with 1 x ESB four times and resuspended in 50 µL ESB. 20% of 5x sample buffer was added and the solution was for 5 min at 95°C. Immunoprecipitations were analyzed by SDS-PAGE and Western blotting as described above.

## **2.8 Animal cap experiments**

Animal cap explants were isolated and treated with activin as described previously (54). Briefly, animal cap explants were isolated from stage 8 embryos and transferred to 1 x MBS in a plasticine-coated dish. Animal caps were then cultured in 0.5 x MBS supplemented with 1:500

of 100x antimycotic (Sigma, Oakville, ON) in the presence or absence of 50 pM activin-A (R&D Systems, Burlington, ON) at 18°C. Sibling embryos were cultured in 0.1 x MBS as a control for normal development. Overnight explant extensions were imaged using a Zeiss Lumar V12 microscope (Zeiss Toronto ON).

## **2.9 Fibronectin Assays**

### *Preparation of FN substrate*

Tissue culture dishes (60 mm) were coated overnight at 4°C with 50 µg/mL of Human plasma fibronectin (FN) (BD Biosciences, Bedford, MA) in PBS (PBS; 130 mM sodium chloride, 3 mM potassium chloride, 10 mM sodium biphosphate, 2 mM monopotassium phosphate).

Substrates were blocked with 1% BSA in PBS and washed twice with 1x MSS (MSS, 3.75 mM sodium chloride, 0.01 mM sodium sulfate, 0.25 mM HEPES, 0.12 mM potassium chloride, 30 mM disodium hydrogen phosphate, 0.07 mM potassium hydrogen phosphate, pH 8.3, supplemented with 1mM calcium chloride and 0.5mM magnesium chloride) before plating cells.

### *Cell Migration Assay*

Animal caps were dissociated in MSS lacking magnesium chloride and calcium chloride, the epidermal ectoderm was removed, and the remaining cells were cultured with 50 pM Activin-A until sibling embryos reached stage 10.5. Dissociated cells were then plated on FN in 1x MSS at low density as described previously (55). Cell migration tracks were recorded for 90 min on a Zeiss Axiovert microscope using Open Lab Software (Perkin Elmer). At least 4 cells per substrate field were followed at 1 min time-lapse intervals.

## 2.10 Immunofluorescence and Microscopy

Antibodies used are listed in Table 2.2.

### *Fibronectin staining*

Control and injected embryos were cultured in 0.1 x MBS until stage 12.5. Embryos were fixed in 2% trichloroacetic acid (TCA) in water for 2 hr at room temperature and then washed twice in 1x phosphate buffer saline (PBS<sup>+</sup>; 130 mM sodium chloride, 3 mM potassium chloride, 10 mM disodium hydrogen phosphate, 2 mM monopotassium phosphate supplemented with 1 mM calcium chloride and 0.5 mM magnesium chloride) with 0.1% Tween 20 (Fisher Scientific, Ottawa, ON). Animal caps were excised in 1x MBS and stained with a monoclonal antibody directed against FN (4B12; 16) in PBS containing 0.1% Tween 20 with 1 ug/mL BSA for 1 hour at room temperature. Primary antibody was detected using Alexa Fluor 546 conjugated goat anti-mouse secondary antibody (Invitrogen, Burlington, ON). Stained animal caps were then mounted on glass slides using 30% glycerol in 1x PBS for imaging.

### *$\beta$ -catenin staining*

Control and injected embryos were cultured in 0.1 x MBS until stage 11. Embryos were then fixed in 4% paraformaldehyde in PBS for 2 hr at room temperature. Embryos were washed three times in 1 x PBS. Animal caps were excised and blocked for 1 hr in PBS containing 0.1% Triton-X and 1  $\mu$ g/ml BSA. Caps were stained with a monoclonal antibody directed against  $\beta$ -catenin (catalogue number C 2206 Sigma, Oakville, ON) for 2 hr at room temperature followed by three washes in 1 x PBS containing 0.1% Triton-X and 1  $\mu$ g/mL BSA and a fourth wash

overnight. Primary antibody was detected by staining with Alexa Fluor 546 conjugated goat anti-mouse secondary antibody (Invitrogen, Burlington, ON) for 2 hr at RT. Stained animal caps were then mounted in 30% glycerol in 1x PBS on glass slides for confocal imaging.

### *Actin staining*

Dissociated animal cap cells cultured with 20 units/mL Activin-A were plated the FN-coated cover slips when sibling embryos reached stage 10.5. Cells were plated until cell boundaries formed between migrating cells. Cells were then fixed with 4% paraformaldehyde in PBS<sup>+</sup> for 30 min. Fixed cells were rinsed with PBS before being permeabilized with PBS<sup>+</sup> with 0.1% Tween 20 (Fisher Scientific, Ottawa, ON). Actin was detected by staining cells with 10 ug/ml rhodamine-phalloidin (Sigma, Oakville, ON) in PBS<sup>+</sup> for 15 min at RT. Cells were rinsed 3 x 20 min with PBS to remove excess rhodamine-phalloidin. Stained cells were mounted in 30% glycerol in PBS on glass slides and imaged using the Zeiss Axiovert 200.

Images of whole embryos and explants were obtained using a Canon PowerShot A620 digital camera or a Zeiss Axiocam mounted on a Zeiss Lumar V12 microscope (Zeiss, Toronto, ON) with Zeiss Axiovision 4 software. Embryonic cells were visualized and cell migrations were monitored using a Zeiss Axiovert 200 inverted microscope (Zeiss, Toronto, ON) equipped with a Ludl motorized stage and Qimaging retiga 1494 digital camera (Qimaging, Burnaby, BC). The images were recorded using OpenLab software (Perkin Elmer; Waltham, MA)

Confocal imaging was carried out using a Nikon Eclipse 90i fitted with a Nikon Eclipse C1 scan head using Nikon NIS elements software (Nikon, Mississauga, ON).

**Table 2: Antibodies**

<b>Antibody</b>	<b>Protein</b>	<b>Dilutions</b>	<b>Supplier</b>
<i>Primary Antibodies</i>			
Anti- $\beta$ -catenin	$\beta$ -catenin	1:1000	Sigma, Oakville, ON
4B12	Fibronectin	1:1000	Gift from Doug W. DeSimone (Ramos and DeSimone, 1996)
GFP (4B10) (mouse monoclonal)	GFP	1:1000	Cell Signaling Tech, Danvers, MA
Anti-GFP from mouse IgG <sub>1</sub> $\kappa$ (clones 7.1 and 13.1)	GFP	1:1000	Roche, Mississauga, ON
ILK1 (4G9)	Integrin-linked Kinase	1:1000	Cell Signaling Tech, Danvers, MA
PINCH-C58	PINCH (Lims1)	1:100 (co-IP) 1:3000 (Western)	Abcam, Cambridge, MA
<i>Secondary Antibodies</i>			
Peroxidase-conjugated Affinipure Goat Antibody	Anti-rabbit IgG, Anti-mouse IgG	1:1000	Jackson Labs, Bar Harbor, ME
Alexa Fluor 546	Anti-mouse IgG, Anti-rabbit IgG	1:1000	Invitrogen, Burlington, ON

## Chapter 3. Experimental Results

### 3.1 Cloning *Xenopus* PINCH

To obtain a full-length cDNA representing *Xenopus laevis* PINCH (referred to as PINCH in this section) I used a previously described expressed sequence tag (EST) that is available in the Genbank database (Genbank Accession # NM01091652 ) to design primers (Table 1) that were used in RT-PCR. The primers were designed to cover the complete open reading frame of the EST. Due to the AT rich sequences found in the 5' region of the PINCH coding sequence I was unable to design a primer that would work in PCR that started at the ATG start codon. Therefore the forward primer encompasses 56 nucleotides upstream of the ATG start site. As these primers were used for all subsequent cloning procedures, all of the PINCH constructs contain a short region upstream of the translation start site (Appendix A, Fig. A4).

Using RNA from stage 12 embryos I generated single strand cDNA that was subsequently used in RT-PCR. The RT-PCR generated a single product of 1080 bp (Fig. 5). This was sub-cloned into pBluescript II SK and sequencing confirmed that it represented a *Xenopus laevis* PINCH ortholog.

PINCH has not been previously described in *Xenopus laevis* and similar to other known PINCH homologs, *Xenopus* PINCH is composed of five LIM domains and has nuclear localization and nuclear export signals (Fig. 6). The amino acid sequence revealed a high identity with human (95.4%), mouse (95.4%), zebrafish (94.5%), and chicken (94.5%) PINCH proteins (Fig. 7A). The sequence diversity between PINCH homologs is summarized as a dendrogram (Fig. 7B).



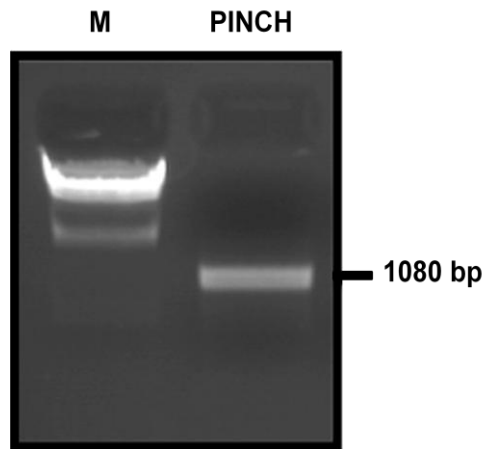


**Figure 5:** *Xenopus laevis* PINCH (PINCH). Total RNA was isolated from stage 12 and first strand cDNA was subjected to RT-PCR using primers listed in Section 2.1. A band at 1080 bp representing PINCH was detected. M, lambda *Hind III* Marker.

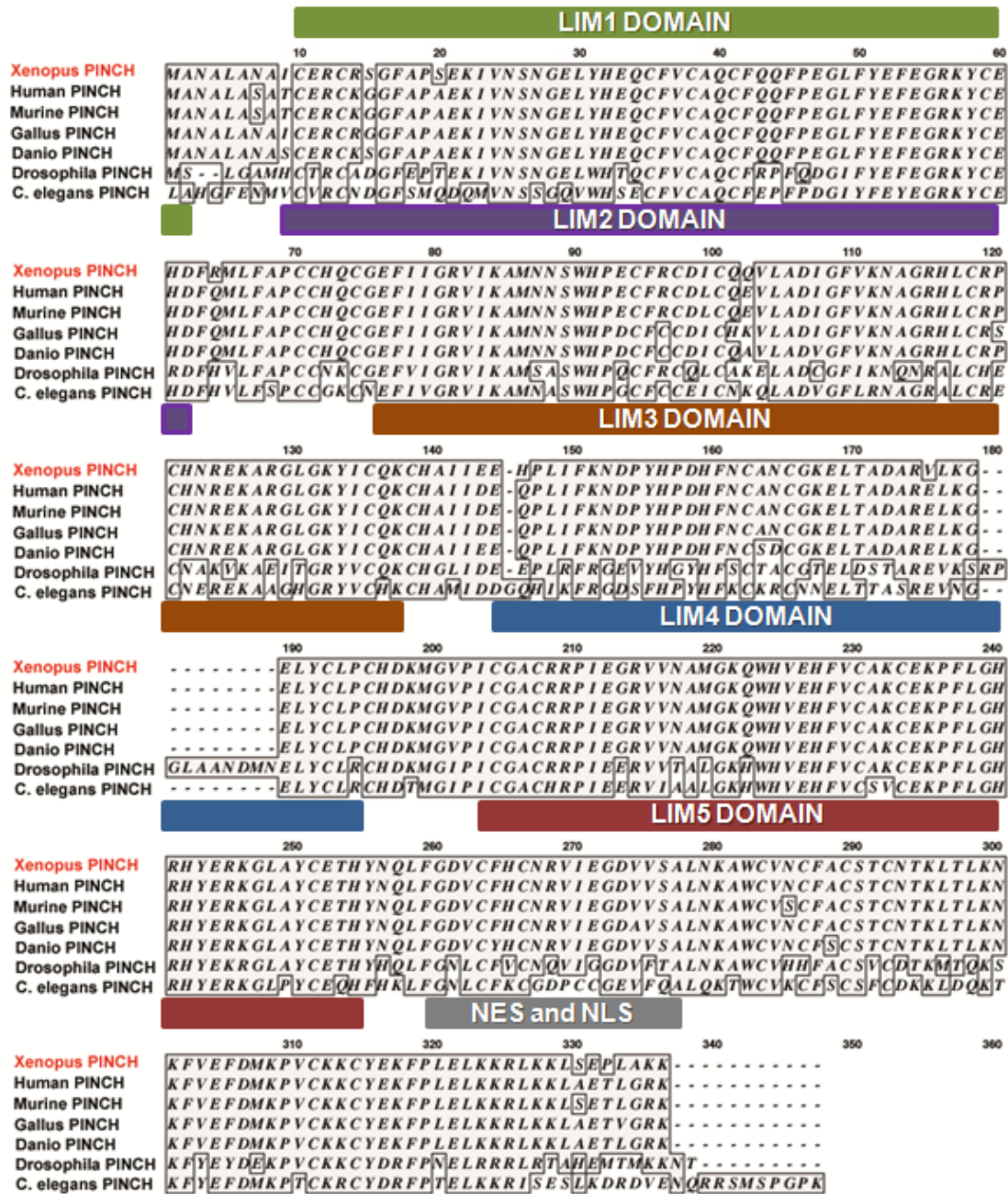
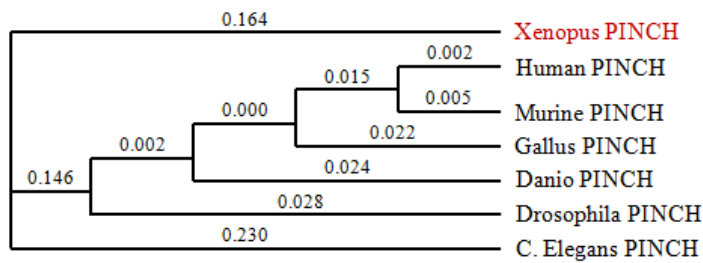


Figure 6: Amino acid sequence alignment of *Xenopus* PINCH and known PINCH orthologs. *Xenopus* PINCH is compared with human, murine, *Gallus*, *Danio*, *Drosophila melanogaster*, and *Caenorhabditis elegans* PINCH orthologs. The LIM domains and nuclear export/localization signals are shown above the amino acid sequences. NES, nuclear export signal; NLS, nuclear localization signal.

**A**

	Percent Identity						
	Xenopus	Human	Mouse	Gallus	Danio	Drosophila	C. elegans
Xenopus		95.4	95.4	94.5	94.5	64.4	57.3
Human	98.2		99.4	96.3	96.0	65.0	57.6
Mouse	97.8	99.7		95.7	95.4	65.0	57.6
Gallus	97.8	98.2	97.8		95.4	64.7	58.2
Danio	97.8	98.5	98.2	98.2		63.5	58.5
Drosophila	78.3	78.9	78.6	78.0	78.0		58.8
C. elegans	76.6	76.0	76.0	76.9	76.6	76.6	

Percent Similarity

**B**

**Figure 7: Comparison of *Xenopus* PINCH with known PINCH homologs.** Sequence distance table comparing percentage identity versus percentage similarity using sequences listed in figure 1. Percent identity is based on the number of identical amino acid pairs in the alignment. Percent similarity is based on the number of identical or similar amino acid pairs divided by the length of the alignment including gaps (“-”) (A). Dendrogram showing the ‘percent divergence’ of the amino acid sequences of *Xenopus* PINCH with known PINCH homologs. Using the protein sequences listed in Figure 5 a dendrogram was prepared using the ClustalW method. The numerical value indicates the divergence between sequences (B).

### 3.2 Temporal and Spatial Expression of PINCH

I used RT-PCR to look at the temporal expression of *Xenopus* PINCH during embryogenesis. In this study, RT-PCR was used as a qualitative assay to determine the expression of PINCH mRNA during early development. PINCH is expressed as a maternal mRNA up to the mid-blastula transition (MBT) (Fig. 8A). PINCH continues to be expressed post-MBT, presumably as a zygotic mRNA from stage 8, through gastrulation (stages 10.5 and 12), neurulation (Stage 17) and at the onset of organogenesis (stage 28) (Fig. 8B).

The spatial localization of *Xenopus* PINCH transcripts was examined by in situ hybridization. PINCH mRNA is expressed in the animal hemisphere of a 2-cell embryo (Fig. 9A; white arrow). Expression is localized to the BCR and the dorsal lip of the early gastrula embryo (Fig. 9B) and persists in the marginal zone in the late gastrula (Fig. 9C). At the neurula stage, there is strong expression in the newly forming somites and the cranial neural crest (Fig. 9D). During the early and late tadpole stages PINCH mRNA is localized to the somite boundaries, head mesoderm, and pharyngeal pouches (Fig. 9E, F).

Since the mesoderm plays an active role in morphogenetic movements (reviewed by (45)), I examined gastrula-stage embryos for PINCH expression in the pre-involution mesoderm tissue. Sagittal sections confirmed mRNA expression initially increases in the BCR and then declines at the onset of gastrulation (Fig. 10A-D, white arrows). During gastrulation *Xenopus* PINCH is expressed in the pre-involution mesoderm of the dorsal and ventral marginal zone (Fig. 10D', white arrow), but is not expressed in the post-involution mesoderm (Fig. 10F', white arrow).

As a commercial antibody to murine PINCH (PINCH C-58; Abcam, Cambridge, MA) was available I further characterized PINCH protein expression using western blots. A 37 kDa band representing PINCH was detected at all stages of development (Fig. 11). A band at 55 kDa was also detected in my western blots. A similar band had been detected previously by others using commercial PINCH antibodies (26). What this band represents is currently unclear. I attempted to use the PINCH antibodies in whole mount immunostaining, however, I was unsuccessful in obtaining a signal.

The experiments described above demonstrate that *Xenopus* PINCH is constitutively expressed throughout early embryogenesis. These observations also indicate that PINCH is expressed in tissues undergoing morphogenetic movements that drive gastrulation.

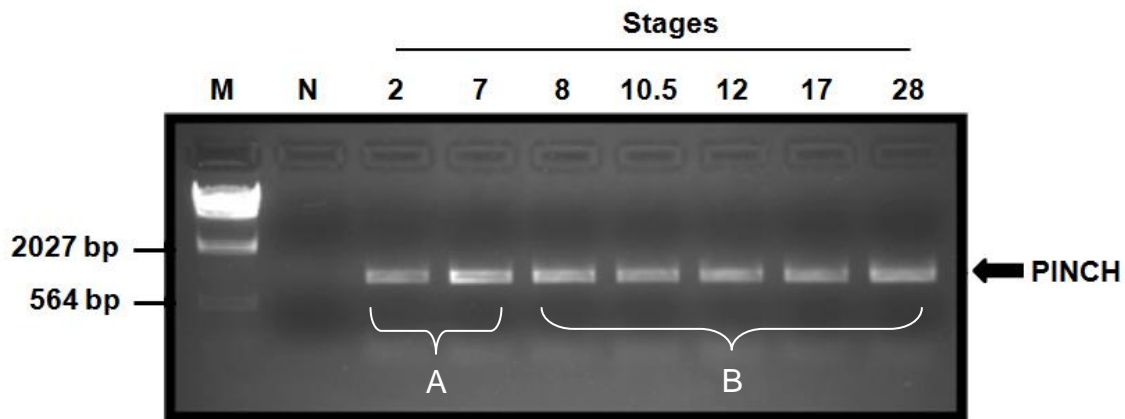


**Figure 8: PINCH mRNA is constitutively expressed throughout early *Xenopus* embryogenesis.** Total RNA was isolated and first strand cDNA from the indicated stages was subjected to RT-PCR using primers listed in Section 2.1. A band at 1080 bp representing PINCH was detected at stages 2, 7, 8, 10.5, 12, 17 and 28. Qualitative analysis indicates that PINCH mRNA is expressed maternally before midblastula transition (MBT) (A) and continues to be expressed zygotically (B). No signal was detected in the absence of cDNA in lane N. M, Marker. N, Negative Control

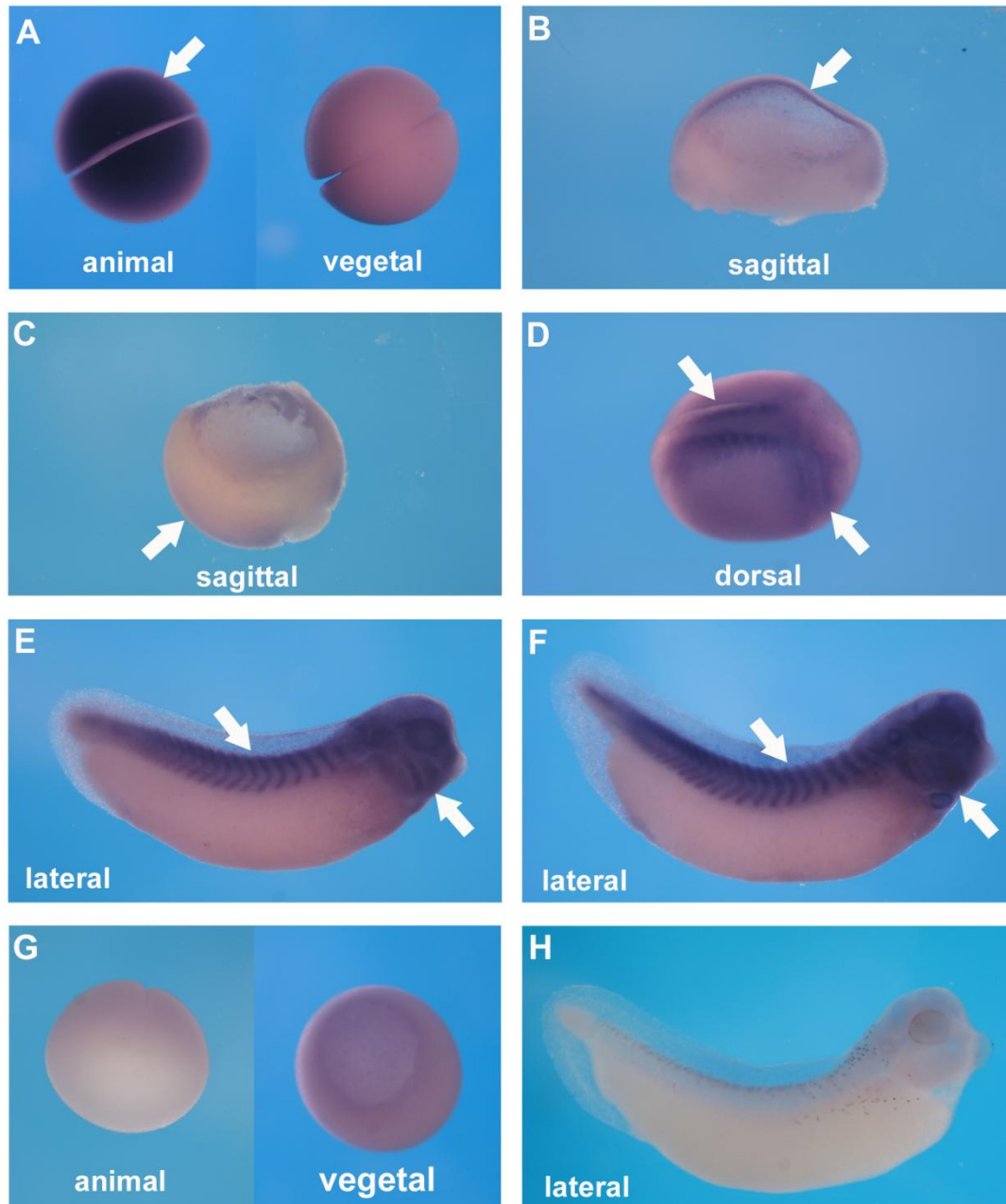


**Figure 9: Spatial Expression of PINCH mRNA during early embryogenesis.** Whole-mount in situ hybridization analysis reveals PINCH mRNA expression at the representative stages. PINCH is expressed in the animal region of a 2-cell embryo (A), in the blastocoel roof and dorsal lip at stage 10.5 (B), in the marginal zone at stage 12 (C), in the somites and cranial neural crest cells at stage 17 (D), and in the developed somites, head mesoderm, and pharyngeal pouches in stage 28 and 36 tadpoles (E, F). PINCH sense probe was used as a negative control (G, H).

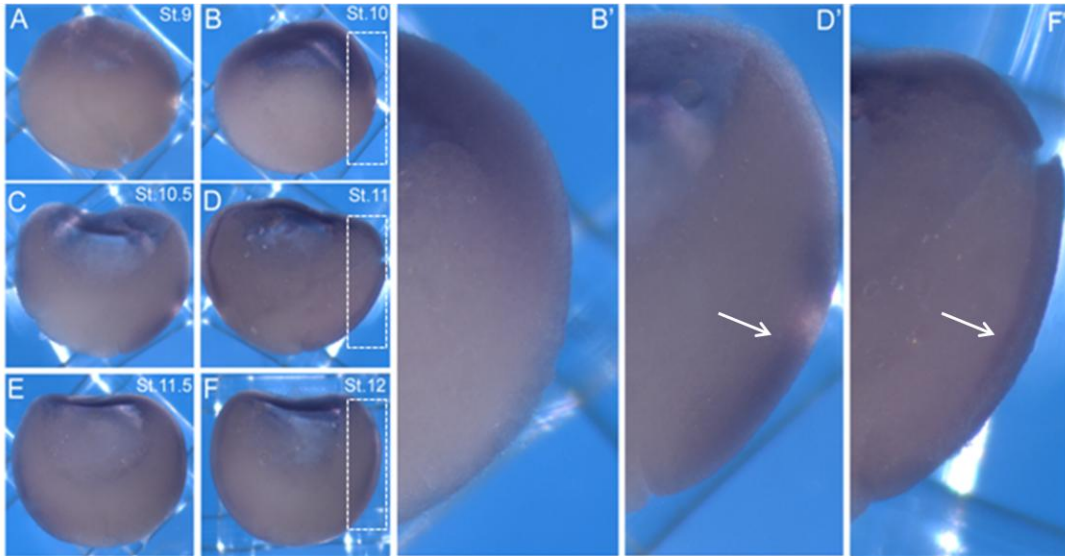


**Figure 10: Spatial Expression of PINCH mRNA during gastrulation.** Whole-mount in situ hybridization analysis reveals PINCH mRNA expression during gastrulation. PINCH mRNA starts to be expressed in the blastocoel roof of a stage 9 embryo (A). At stage 10, there is strong expression in the blastocoel roof (B). From stages 10.5-11, expression diminishes in the blastocoel roof but increases in both the dorsal and ventral marginal zones (C, D). Expression in the marginal zone persists through stages 11.5 to 12 (E, F). PINCH starts to be expressed in the pre-involution mesoderm at the onset of gastrulation (D', white arrow), but does not persist in post-involution mesoderm (F', white arrow).



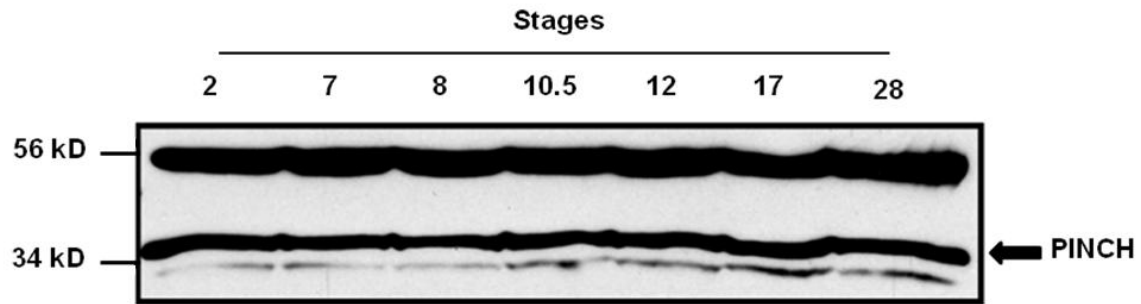


**Figure 11: PINCH protein is constitutively expressed during early embryogenesis.** Western Blot analysis reveals a 37 kDa band, as expected for PINCH, at all the representative stages. The ~55 kDa band represents a non-specific association.

### 3.3 PINCH and *Xenopus* gastrulation

#### 3.3.1 Characterization of PINCH LIM domains

At the onset of this project the only two known binding partners of PINCH were Integrin-Linked Kinase (ILK) and Grb4 (21, 32). I used site directed mutagenesis to generate amino acid substitutions that have previously been shown to abolish function in the LIM1 and LIM4 domains (57-58). These constructs are referred to as LIM1<sub>mut</sub> and LIM4<sub>mut</sub> respectively. The mutations were confirmed by sequencing (Appendix A). *Xenopus* kidney epithelial A6 cells were transfected with a plasmid encoding GFP-tagged PINCH to verify the expected localization of the construct *in vitro* (Fig.12). GFP-PINCH localizes to the nucleus and to focal adhesions similar to what has been described previously in mammalian cell lines (59) (Fig. 12A). The change of the AQCF sequence in the LIM1 domain to AACF was previously shown to abolish interactions with ILK and localization to focal adhesions in mouse C2C12 cells (57). However, this mutation in PINCH has no effect on the localization of GFP-LIM1<sub>mut</sub> to focal adhesions in A6 cells (Fig. 12B). The double R197A-R198A mutation in the LIM4 domain was previously shown to inhibit binding with Grb4 (58). This mutation in PINCH has no effect on the localization (Fig. 12C). Together, these observations suggest that the LIM1 and LIM4 domains are not involved in the localization of PINCH to focal adhesions in A6 cells and that the GFP tag has no effect on PINCH localization.

#### 3.3.2 Examining a role for PINCH in *Xenopus* gastrulation

In *Xenopus* embryos one of the hallmarks of gastrulation is the progressive closure of the blastopore. Blastopore closure has been shown to be an integrin dependent process and since PINCH is thought to regulate integrin signalling I looked at the effect of PINCH over-

expression on blastopore closure (Fig. 13). Control embryos exhibited normal blastopore closures during mid-gastrulation, indicating proper progression of gastrulation (Fig. 13A). A GFP control was included showing that the GFP tag has no effect on blastopore closures (Fig. 13B). Over-expression of PINCH mRNA showed a delay in blastopore closures at concentrations of 1 ng (C), 2 ng (C'), and 4 ng (C'') injected mRNA. Over-expression of LIM1<sub>mut</sub> mRNA resulted in no observable effect at 1 ng (D) and 2 ng (D'), but exhibited a delay in blastopore closures at 4 ng injections (D''). In contrast, over-expression of LIM4<sub>mut</sub> mRNA has a potent affect on blastopore closures at 2 ng (E') and 4 ng (E''). The difference in phenotype between constructs is not due to difference in expression levels as protein expression levels are similar for all constructs (Fig. 14). As mutations in the LIM1 and LIM4 domains relieve inhibition of blastopore closures it is likely that over-expressing full length PINCH is titrating out proteins that interact with these domains that are essential for gastrulation.

It has previously been shown that mesoderm patterning and the cell movements of gastrulation can be dissociated. To test if the failure of gastrulation stems from tissue patterning or a failure in morphogenesis I looked at mesoderm patterning in embryos expressing the PINCH constructs. In situ hybridization was performed using the mesodermal marker *brachyury* (*Xbra*), which identifies pre-involution mesoderm and post-involution notochord (Fig. 15A, A') (60). Two ng of PINCH, LIM1<sub>mut</sub>, and LIM4<sub>mut</sub> mRNA were microinjected into embryos for over-expression analysis. Over-expression of PINCH results in delay in blastopore closures (Fig. 15B). Sagittal sections reveal that *Xbra* is expressed in the pre-involution mesoderm and that involution at the dorsal lip has likely failed resulting in no extension of the axial mesoderm (Fig. 15B'). Over-expression of LIM1<sub>mut</sub> (Fig. 15C, C') and LIM4<sub>mut</sub> (Fig. 15 D, D') show a similar result, indicating that PINCH regulates cell movements and not mesoderm patterning.

The cell movements of epiboly in the BCR are known to contribute to the cell rearrangements that drive gastrulation (Section 1.1). Because PINCH over-expression disrupts morphogenesis, I asked whether PINCH has an effect on cell intercalation behaviour driving epiboly. Before the onset of gastrulation, the *Xenopus* BCR is three to four cell layers thick in the animal region of the embryo (61). As development progress, the cell layers rearrange into two layers by cell intercalation movements. I examined the BCR thickness in bisected embryos at stage 12.5 (late gastrulation) (Fig. 16). Embryos injected with GFP-tagged PINCH, LIM1<sub>mut</sub>, and LIM4<sub>mut</sub> show a thicker BCR compared to non-injected embryos indicating that epiboly has failed in these embryos. Compared to PINCH and LIM1<sub>mut</sub> expressing BCRs, BCRs expressing LIM4<sub>mut</sub> appear to be looser suggesting a difference in deep layer cell cohesion.

Together, these results indicate PINCH over-expression does not affect mesoderm patterning; specifically PINCH does not inhibit the transcription of immediate early gene *Brachyury*. Moreover, the gastrulation defects appear to be caused by a direct interference with cell movements driving gastrulation.

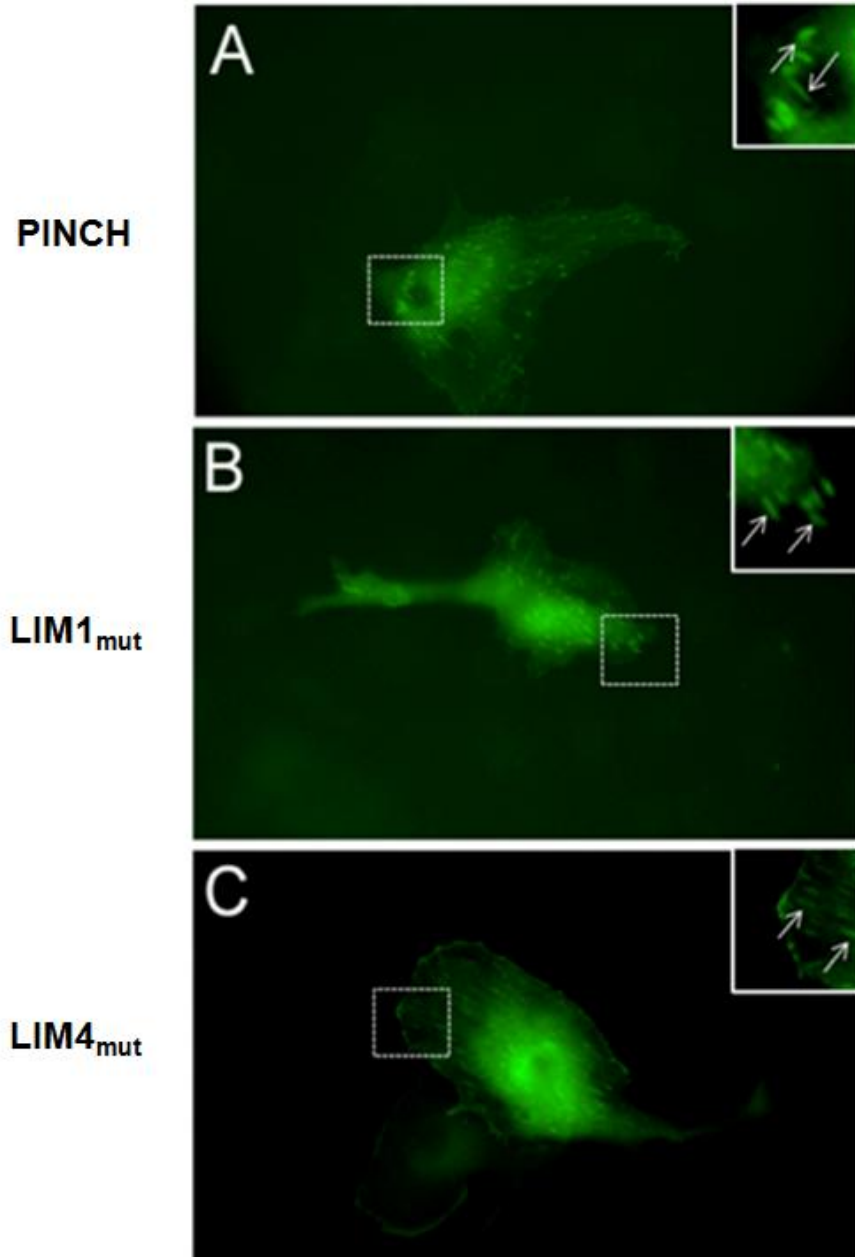


**Figure 12: GFP-tagged PINCH constructs localize to focal adhesions in *Xenopus* A6 kidney cells**  
GFP-tagged PINCH localizes to the nucleus and focal adhesions (A). The LIM1<sub>mut</sub> construct leads to the same phenotype despite disrupting the expected interaction between PINCH and ILK (B). Abolishing the potential binding between PINCH and Grb4 has no effect on PINCH localization to focal adhesions (C). Insets show magnified views of the boxed regions. White arrows indicate the focal adhesion structures.

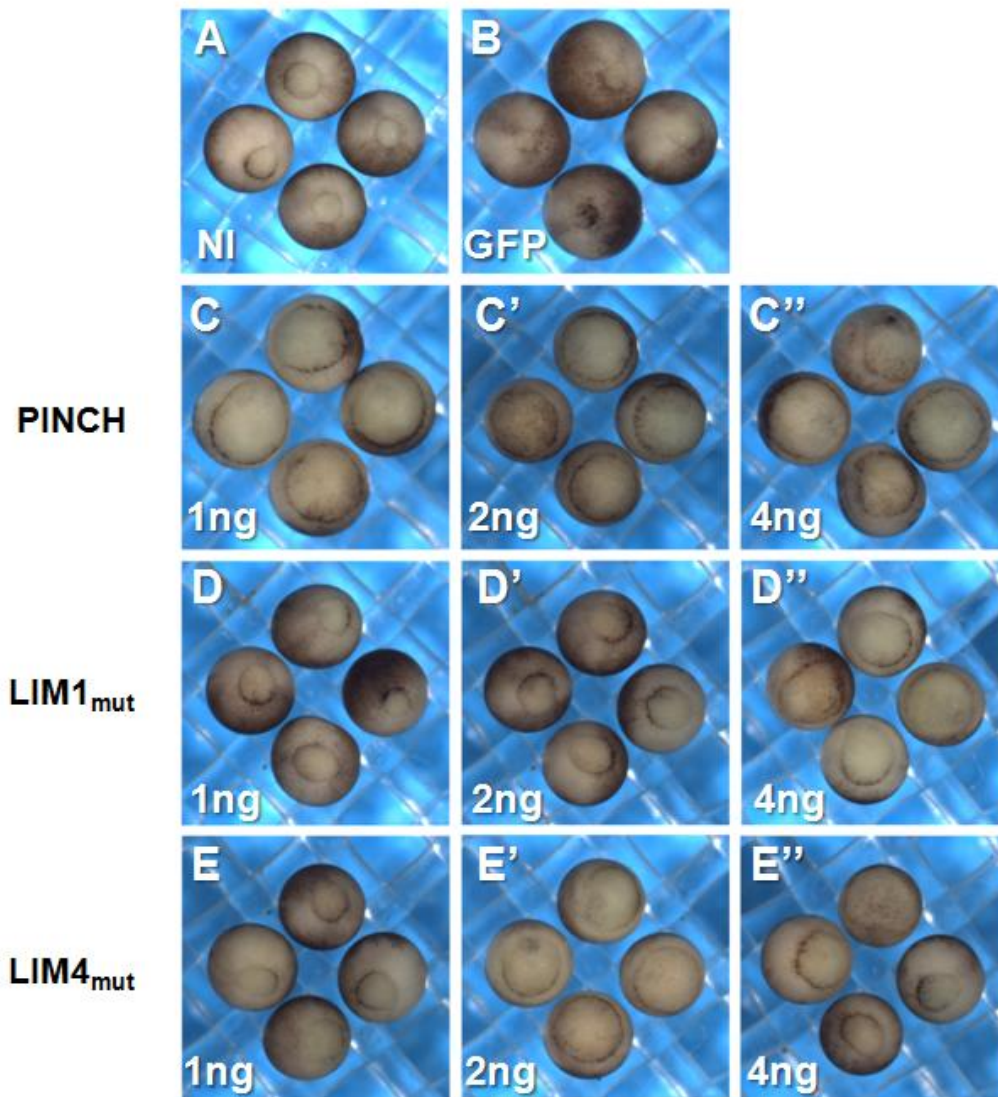


**Figure 13: Over-expression of PINCH delays blastopore closures.** RNA was microinjected into the animal cap of a 2-cell embryo and blastopores were viewed at stage 12. PINCH over-expressing embryos show a delay in blastopore closures at 1 ng (C), 2 ng (C'), and 4 ng (C'') microinjections. LIM1<sub>mut</sub>-expressing embryos displays normal blastopore closures at 1 ng (D) and 2 ng (D') and potent at 4 ng (D'') while over-expression of LIM4<sub>mut</sub> shows a delay in blastopore closures at 2 ng (E') and 4 ng (E''). The weaker effect at lower concentrations in both LIM1<sub>mut</sub> (D, D') and LIM4<sub>mut</sub> (E) embryos indicate the functional importance of both LIM1 and LIM4 domains. Blastopore diameters are highlighted in red. NI, Non-injected control.

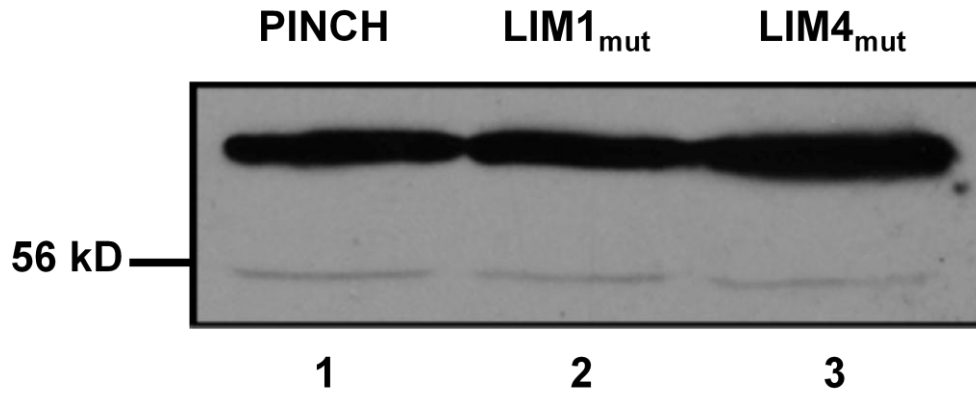


**Figure 14: Protein expression in embryos microinjected with PINCH mRNA.** Western Blot Analysis reveals a 64 kDa band representing GFP-tagged PINCH (lane 1), LIM1<sub>mut</sub> (lane 2), and LIM4<sub>mut</sub> (lane 3). All lanes show approximately equal protein expression in injected embryos. Each lane represents approximately 3 embryo equivalent.

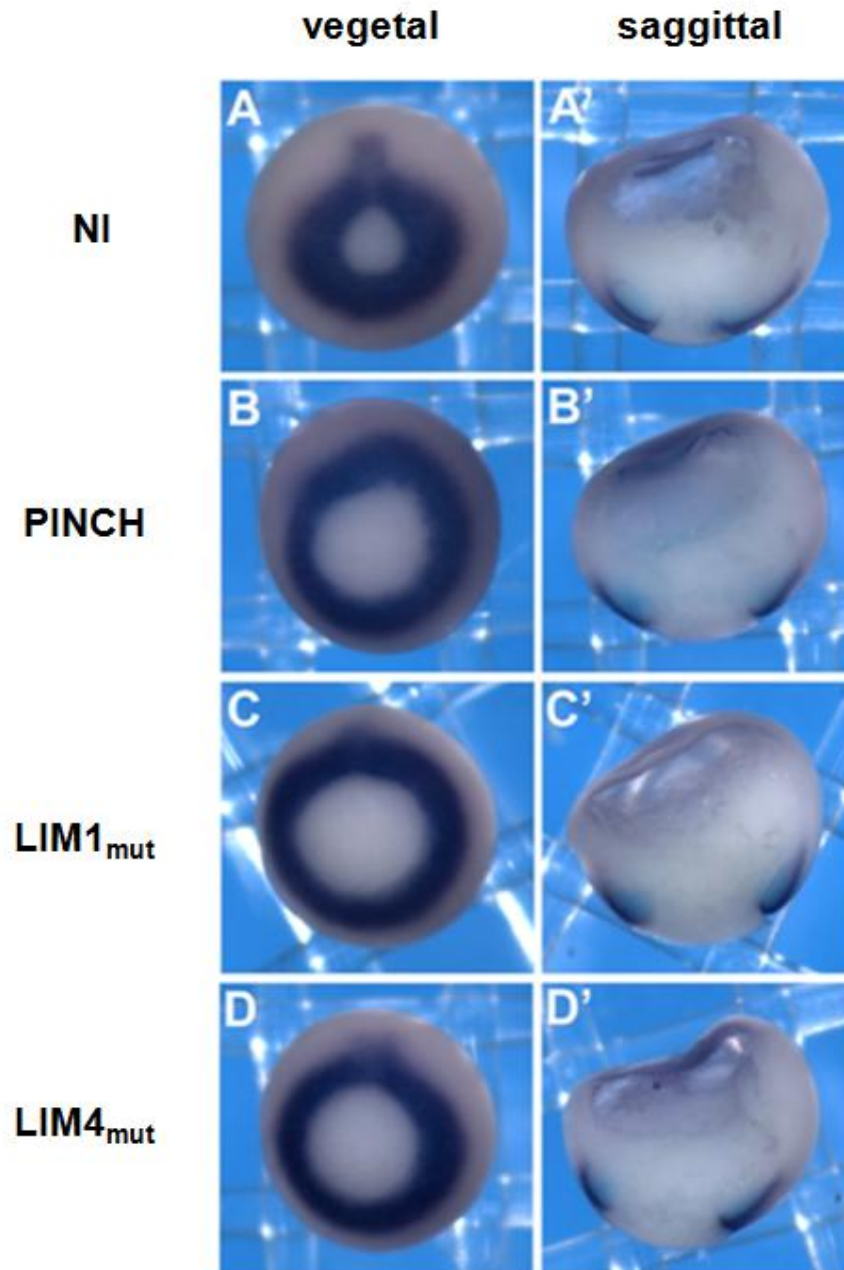


**Figure 15: PINCH over-expression does not affect mesodermal patterning.** In situ hybridization against *Brachyury* reveals the pre-involution mesoderm and post-involution notochord in Non-injected (NI) embryos (A, A'). Over-expression of PINCH (B), LIM1<sub>mut</sub> (C) and LIM4<sub>mut</sub> (D) show a delay in blastopore closures and failure in axial extension. However, mesodermal patterning is not affected in embryos (B', C', D')



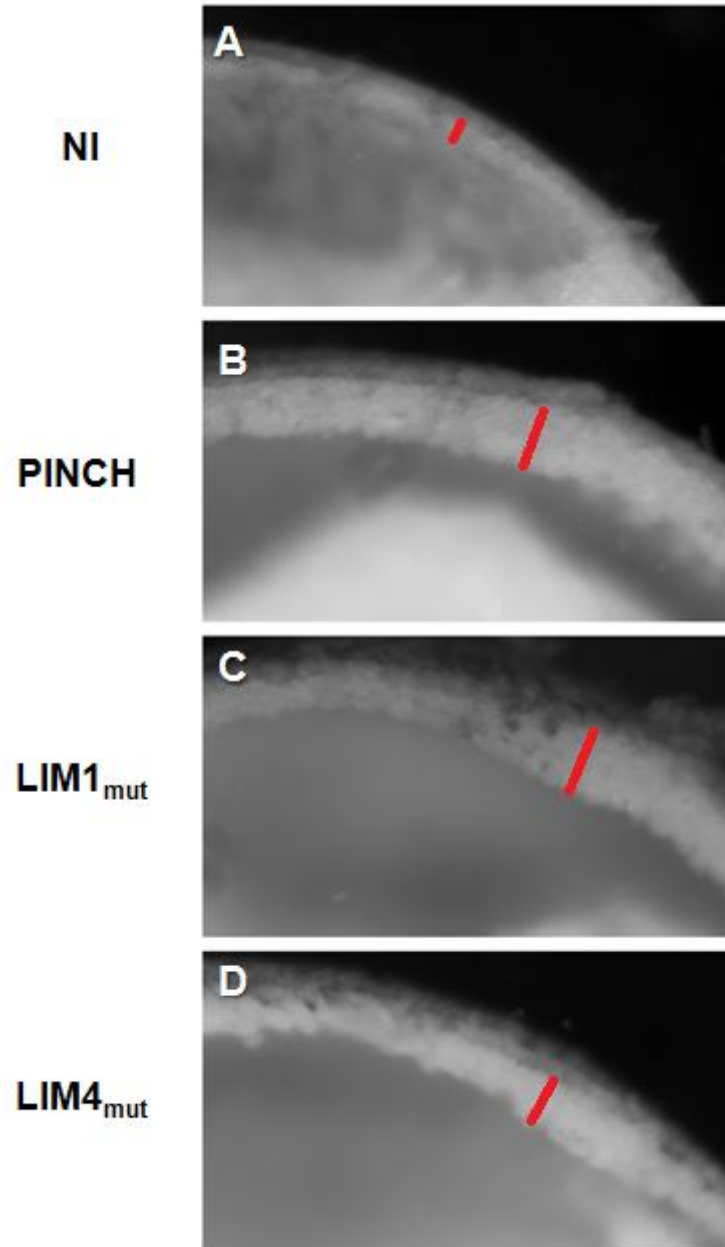


**Figure 16: PINCH controls epiboly in the BCR.** Sagittal sections of stage 12 gastrula embryos. In all panels embryos are arranged with the dorsal lip towards the right. There is only a 2 cell layer of deep cells in the BCR of stage 12 embryos (A). BCRs from embryos expressing PINCH (B), LIM1<sub>mut</sub> (C), and LIM4<sub>mut</sub> (D) have multiple layers of deep cells. The red bars represent the thickness of the blastocoel roof.

### **3.4 PINCH and FN matrix assembly**

#### **3.4.1 PINCH over-expression inhibits FN matrix assembly**

It is well established that a FN matrix lining the blastocoel roof is essential for the cell movements that drive epiboly. As PINCH over-expression caused a failure in epiboly I asked if this was related to FN matrix assembly.

RNA injections targeted the animal pole of two-cell embryos and the blastocoel roof was examined for a FN matrix at stage 12.5. BCRs isolated from non-injected control embryos display a typical mature FN matrix comprising of long, dense, and organized fibrils (Fig. 17A, NI). Embryos microinjected with GFP as a control for the GFP tag displayed a similar FN matrix (Fig. 17B). Explants over-expressing PINCH and LIM1<sub>mut</sub> fail to assemble fibrils into a mature matrix (Fig. 17C, D). However over-expression of LIM4<sub>mut</sub> results in a lesser inhibition of FN matrix assembly (Fig. 17E). The presence of sparse fibrils in these explants suggests that PINCH is likely involved in the assembly of the fibrils into an organized matrix and that the LIM4 domain plays an important role in this process.

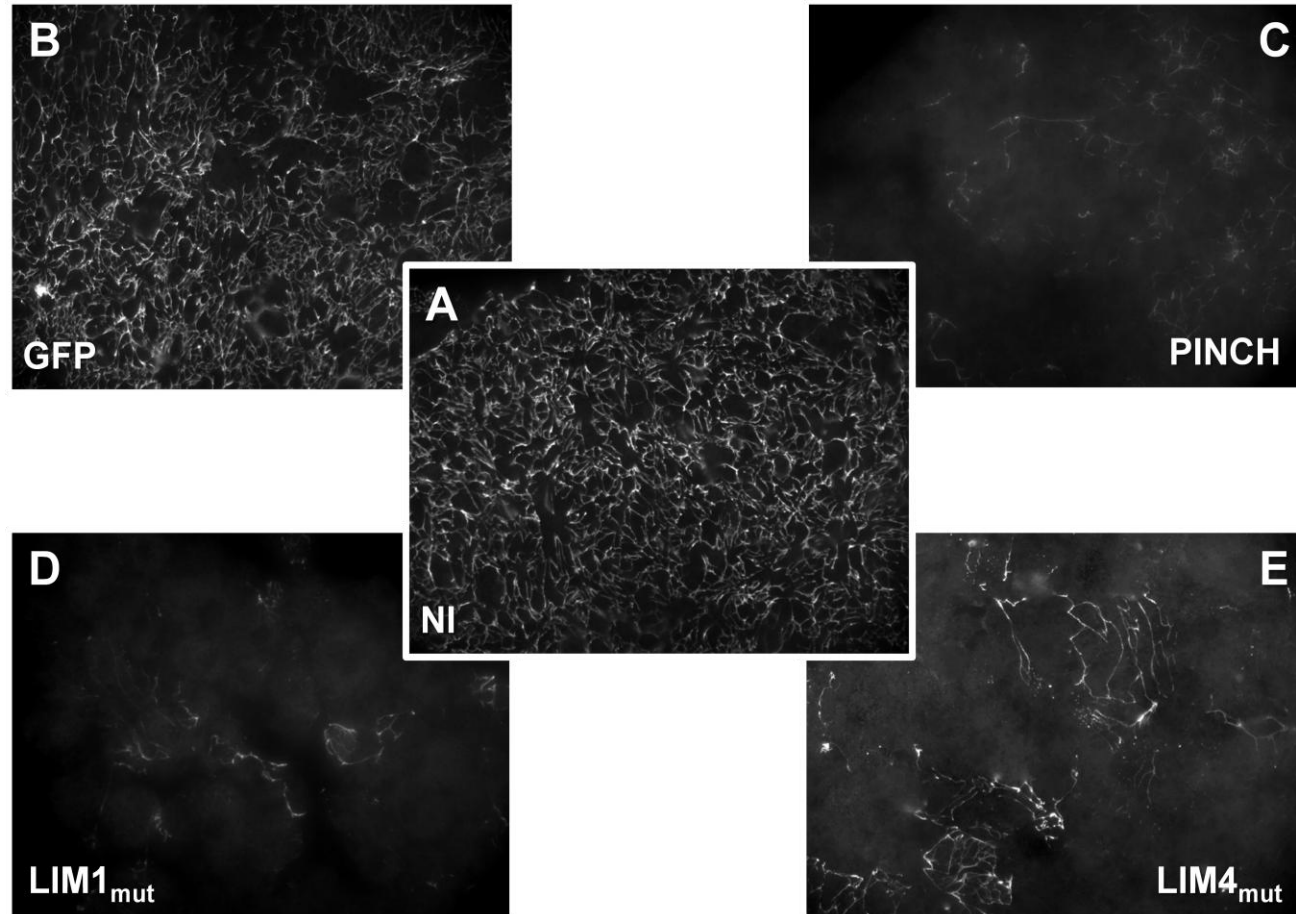


**Figure 17: PINCH is required for FN matrix assembly.** FN matrix assembly on the BCRs of stage 12.5 embryos was detected using Immunofluorescence. The staining of non-injected (A) and GFP-injected (B) BCRs showed an elaborate FN matrix. Embryos microinjected with GFP-tagged PINCH (C) and LIM1<sub>mut</sub> (D) mRNA severely inhibited FN fibril formation across the BCR. BCRs expressing GFP-tagged LIM4<sub>mut</sub> (E) show a lesser inhibition of FN matrix assembly than PINCH and LIM1<sub>mut</sub> and the presence of longer fibrils. NI, Non-injected control.

### 3.4.2 PINCH and Integrin Adhesion

Cells lining the BCR use  $\alpha 5\beta 1$  integrin to bind and assemble FN. I therefore investigated if over-expressing PINCH interferes with FN matrix assembly through mis-regulation of  $\alpha 5\beta 1$  integrin.

Treatment of stage 8 animal cap cells with activin induces a mesodermal fate and cells acquire the ability to spread and migrate on FN. This change in adhesive behaviour has been suggested to be a result of  $\alpha 5\beta 1$  integrin activation (15). To examine the role that PINCH may play in integrin mediated cell adhesion isolated animal cap cells were treated with 50 pM activin and plated on FN. Cells were counted, the dish rinsed lightly to remove non-adherent cells, and cells counted post-wash to obtain an estimate of the cell adhesion. The results are presented in Figure 18. Compared to control, 93.6%  $\pm 0.14\%$  of PINCH expressing cells attach and spread on FN. In contrast, 92.3%  $\pm 0.10\%$  of LIM1<sub>mut</sub> and 104.8%  $\pm 0.07\%$  of LIM4<sub>mut</sub> expressing cells attach on FN. However, the differences seen in PINCH, LIM1<sub>mut</sub>, and LIM4<sub>mut</sub> expressing cells are not statistically significant compared to control ( $P > 0.05$ , Student T-test), indicating all cells have a similar affinity to FN. A single tailed T-test was used to look at significance between control samples and test samples. Test samples were not compared with each other. My results suggest that PINCH does not play a role in modulating adhesion of cells to FN through the  $\alpha 5\beta 1$  integrin receptor.

As integrin behaviour is altered through inside out signalling following activin exposure I asked if PINCH plays a role in activin-induced migration. Isolated animal cap cells were treated with activin, plated on FN and individual migration tracks were recorded (Fig. 19A). Compared to control cells, PINCH, LIM1<sub>mut</sub>, and LIM4<sub>mut</sub> expressing cells show similar migration patterns. The total distances travelled by PINCH, LIM1<sub>mut</sub>, and LIM4<sub>mut</sub> expressing

cells were recorded and graphed as a percentage of distance travelled by control cells (Fig. 19B). Cells expressing microinjected PINCH mRNA travel an average of  $98.5\% \pm 0.15\%$  compared to control cells from non-injected embryos. In contrast, cell expressing LIM1<sub>mut</sub> and LIM4<sub>mut</sub> migrate an average of  $102.0\% \pm 0.19\%$  and  $91.2\% \pm 0.11\%$  compared to control cells. A single tailed T-test was used to compare control samples with test cases. The differences seen in migration distances are not statistically significant compared to control cells ( $P > 0.05$ , Student T-test). My results indicate that the LIM1 and LIM4 domains are not required for activin induced changes in  $\alpha 5\beta 1$  integrin-mediated migration on FN.

As cell intercalation requires the ability of  $\alpha 5\beta 1$  integrin to transmit a signal from FN into the cell, I used animal cap extension assays to determine if PINCH regulates outside-in integrin signalling. Ectoderm explants that encompass the animal cap of the blastula heal into round balls when cultured overnight in 0.5 x MBS (Fig. 20A). When cultured in the presence of 50 pM activin explanted animal caps elongate recapitulating the cellular movements of convergent extension (Fig. 20B). Animal caps isolated from embryos that have previously been injected with an mRNA encoding GFP were used as a control for non-specific effects of the injection procedure. These explants extend in the presence of activin similar to animal caps isolated from un-injected embryos (Fig. 20 C, D). Animal caps expressing PINCH (Fig. 20F) and LIM1<sub>mut</sub> (Fig. 20H) elongate in the presence of activin. Animal caps expressing the LIM4<sub>mut</sub> construct, however, do not extend in the presence of activin, indicating a failure in convergent extension movements (Fig. 20 I, J). None of the explants extend in the absence of activin demonstrating that PINCH is not permissive for cap extension. GFP-tagged constructs were confirmed to be expressed in tissues undergoing convergent extension (Fig. 20 E'- J').

In cultured cell models PINCH is an obligate partner with ILK in the IPP complex (20). Because PINCH is not required for integrin function in the gastrula, I asked if PINCH is still binding to ILK and functioning as part of an IPP complex. I used a co-immunoprecipitation assay (co-IP) to determine if PINCH interacts with ILK in the embryo. PINCH was immunoprecipitated with PINCH-C58 antibody and the immunoprecipitates were then separated. The presence of ILK as a co-immunoprecipitate was revealed using ILK1 antibody. ILK is present in embryo lysates (Figure 20, lane 1, arrow). However ILK is not present in PINCH immunoprecipitates (Figure 21, lane 2) indicating that the IPP complex may not exist in *Xenopus* embryos. A protein band, of higher molecular weight than ILK, was detected in the pull-down lane (Figure 21, lane 2) and likely represents the IgG heavy chain.

Together, these data show that PINCH does not affect integrin-mediated cell adhesion or migration and is unlikely to be part of an IPP complex that participates in the integrin signalling pathway.

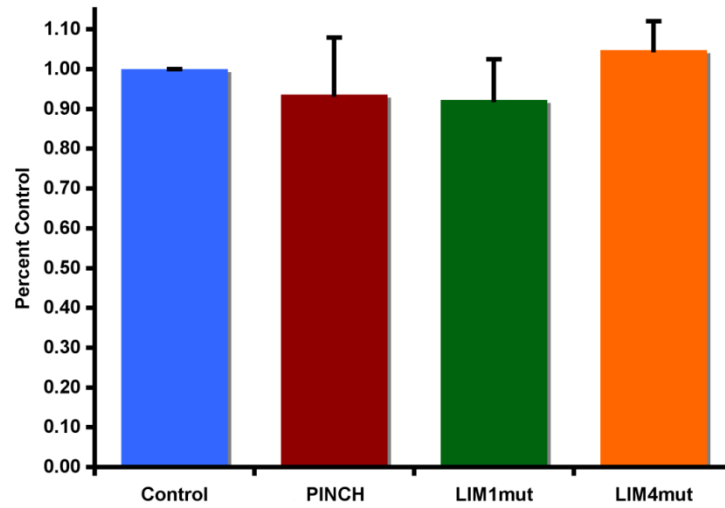


**Figure 18: Quantification of activin-treated cell adhesion to FN substrates.** Cells were treated with activin and plated on FN substrates. Cells that attached and spread were counted pre-wash and post-wash. The values for each construct are presented as a percentage of the control cells that attached and spread on FN. Control, PINCH, LIM1<sub>mut</sub>, and LIM4<sub>mut</sub> show similar affinity for FN. Data represents 3 experiments, N=12.

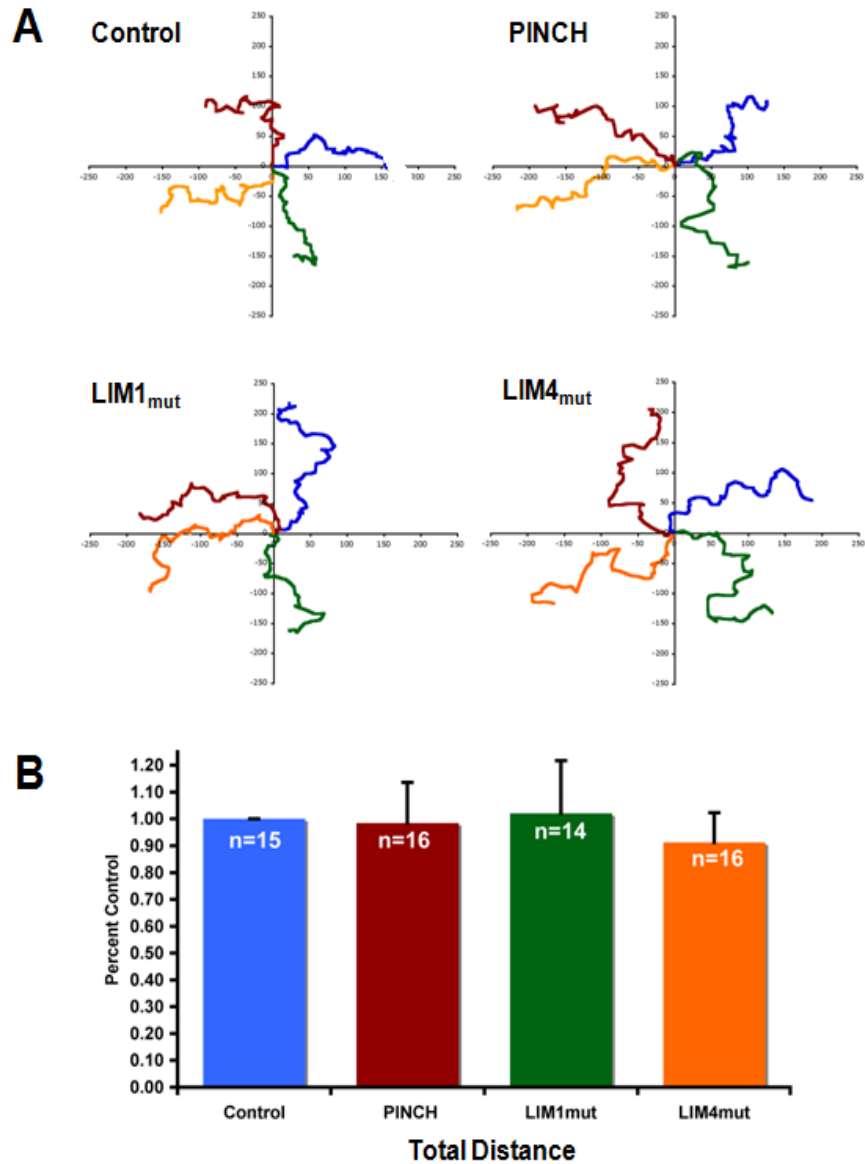


**Figure 19: PINCH does not affect activin-induced cell migration.** (A) Spider graphs representing migration tracks of individual activin-induced cells plated on FN substrates. Each graph contains 4 representative tracks with start point set at (0, 0). Horizontal and vertical scale is in  $\mu\text{m}$ . There is no difference in migration patterns when comparing control, PINCH, LIM1<sub>mut</sub>, and LIM4<sub>mut</sub> over-expressing cells. (B) Percent control of the total distance of activin-treated cells on FN substrates. Measurements are from the same cells represented in (A). Cells derived from control non-injected embryos and PINCH, LIM1<sub>mut</sub>, and LIM4<sub>mut</sub> over-expressing cells travel similar distances. Data represents 3 experiments (standard errors determined using N values listed).



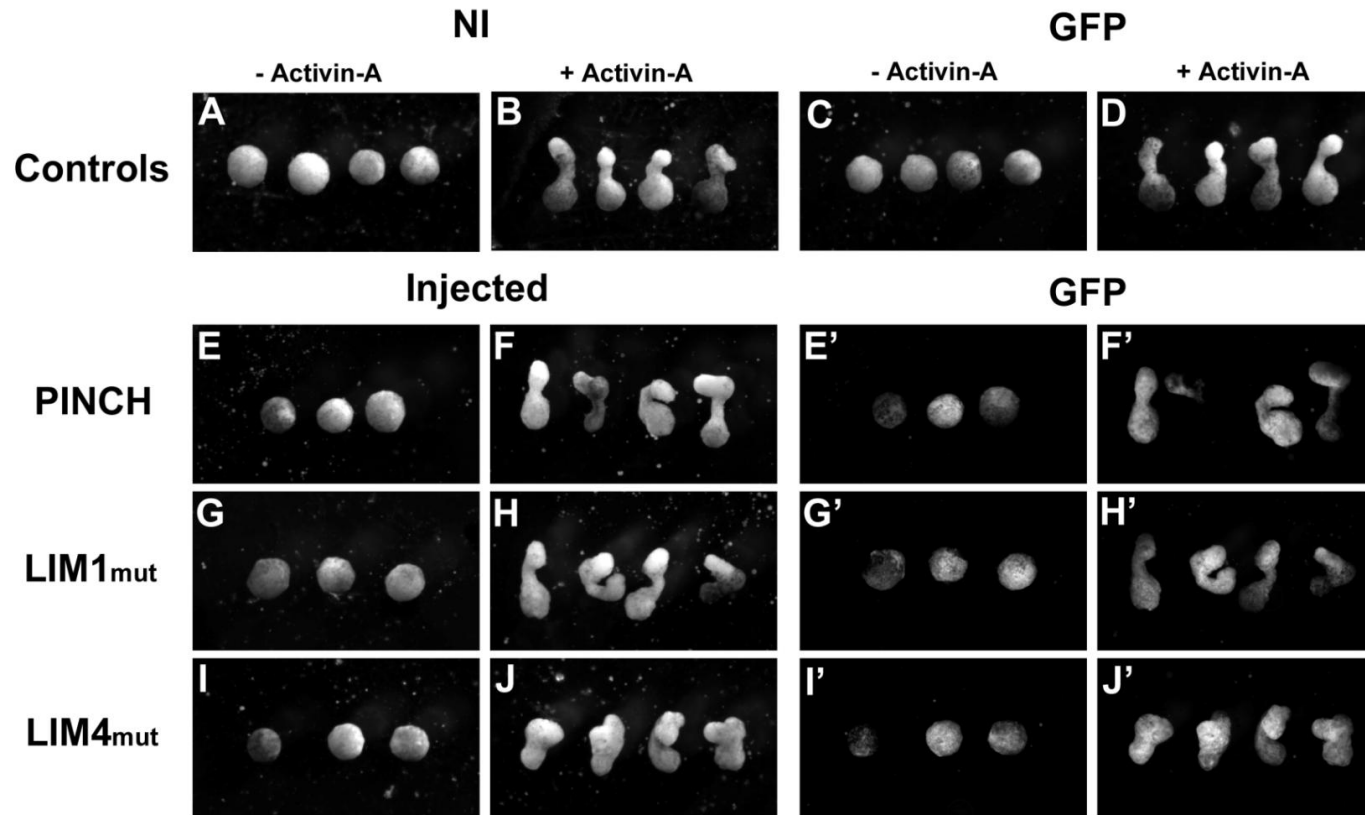


**Figure 20: PINCH is not permissive for convergent extension.** Stage 8 animal caps were cultured in the presence or absence of activin-A, until sibling embryos reached stage 18. Induced explants from non-injected embryos (B), GFP-injected embryos (D), PINCH-injected (F), and LIM1<sub>mut</sub>-injected (H) embryos elongated. Expression of LIM4<sub>mut</sub> inhibits animal cap elongation, indicating a failure in convergent extension (J). Uninjected LIM4<sub>mut</sub> expressing explants did not elongate (I). Sibling explants did not extend in the absence of activin-A induction (A, C, E, G, H). GFP expression was consistent in explants expressing PINCH (E', F'), LIM1<sub>mut</sub> (G' H'), and LIM4<sub>mut</sub> (I', J'). NI, Non-injected control.

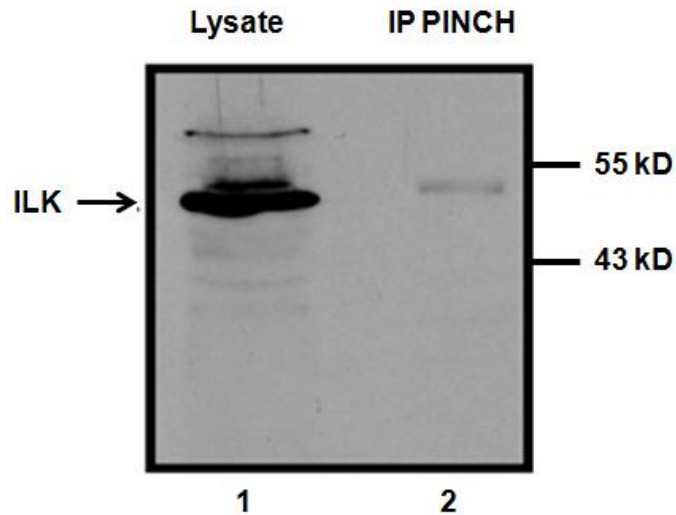


**Figure 21: PINCH is unlikely to interact with ILK *in vivo*.** PINCH was immunoprecipitated with a PINCH-C58 antibody. The presence of ILK as a co-immunoprecipitate was examined using an ILK1 antibody. Co-immunoprecipitation analysis shows that ILK does not co-immunoprecipitate with PINCH. A 54 kDa band representing ILK is present in the lysate (Lane 1). ILK was not detected in PINCH immunoprecipitates with PINCH-C58 antibody (Lane 2).

### 3.4.3 PINCH and Cadherin Adhesion

The inhibition of FN matrix assembly observed in embryos that are over-expressing PINCH does not appear to be mediated through changes in integrin adhesion or signalling. A possible alternative explanation is that PINCH interferes with cadherin-mediated adhesion in the cells lining the BCR.

To examine a possible role for PINCH in regulating C-cadherin mediated cell-cell adhesion, animal cap cells were plated on FN and localization was monitored in cells that touch each other. GFP-tagged PINCH showed accumulation at nascent sites of cell-cell adhesion (Fig. 22A, white arrow)). GFP-tagged LIM1<sub>mut</sub> and LIM4<sub>mut</sub> showed a similar localization suggesting that LIM1 or LIM4 domains are not required for this localization (Fig. 22B, C; white arrows). Because C-cadherin function is known to be regulated in the BCR during FN assembly (62), I asked if PINCH modulates the function of C-cadherin *in vivo*.

Initial experiments addressed if the localization of PINCH to sites of cell-cell adhesion in isolated cells also occurred in the embryo. BCRs from GFP, PINCH, LIM1<sub>mut</sub>, and LIM4<sub>mut</sub> expressing embryos were stained for an adherens junction marker  $\beta$ -catenin (Fig. 23B, D, F, and H). As expected, GFP does not co-localize with  $\beta$ -catenin at cell boundaries (Fig. 23 A-C). BCRs from GFP-tagged PINCH expressing embryos showed strong PINCH localization to cell-cell boundaries where it co-localizes with  $\beta$ -catenin (Fig. 23D-F). BCRs expressing LIM1<sub>mut</sub> (Fig. 23 G-I) and LIM4<sub>mut</sub> (Fig. 23 J-L) display a similar co-localization, suggesting the LIM1 and LIM4 domain is not required for PINCH localization to cell boundaries *in vivo*.

Because PINCH localizes with  $\beta$ -catenin at adherens junctions, I next asked if the failure in FN matrix assembly in PINCH expressing embryos is linked to changes in cell-cell adhesion. The change in shape of BCR cells from round to polygonal over the course of gastrulation has

been attributed to the maturation of adherens junctions and an increase in tissue tension (13). Compared to the polygonal cells in BCRs expressing PINCH (Fig. 23F), BCRs expressing LIM1<sub>mut</sub> (Fig. 23I) and LIM4<sub>mut</sub> (fig. 23J) contain larger rounded cells suggesting a decrease in tissue tension. Vertical confocal sections of control BCRs show typical localization of adherens junctions at the apical surface (Fig. 24A, blue arrows). In contrast the adherens junctions appear to shift basally in BCRs expressing PINCH, LIM1<sub>mut</sub> and LIM4<sub>mut</sub> (Fig. 24B, C, D; blue arrows). The overlapping cells in these BCRs are consistent with previous results showing an increase in BCR thickness (Fig. 24, dotted boxes). These observations suggest either a disruption of cell intercalation movements or the inability of cells to maintain proper organization along the inner BCR.

Because PINCH over-expression phenotypes show a possible reduction in cell-cell adhesion across the BCR, I asked if this could be attributed directly to a change in cadherin mediated adhesion. Isolated animal cap cells were plated on a substrate consisting of the extracellular domain of C-Cadherin (FcCad; 63). Cells were allowed to attach to the substrates, counted, rinsed lightly and cells were counted post-wash. PINCH, LIM1<sub>mut</sub>, and LIM4<sub>mut</sub> expressing cells all show similar affinity for cadherin and did not vary significantly from control (Fig. 25). These results indicate that PINCH does not influence C-cadherin mediated cell adhesion.

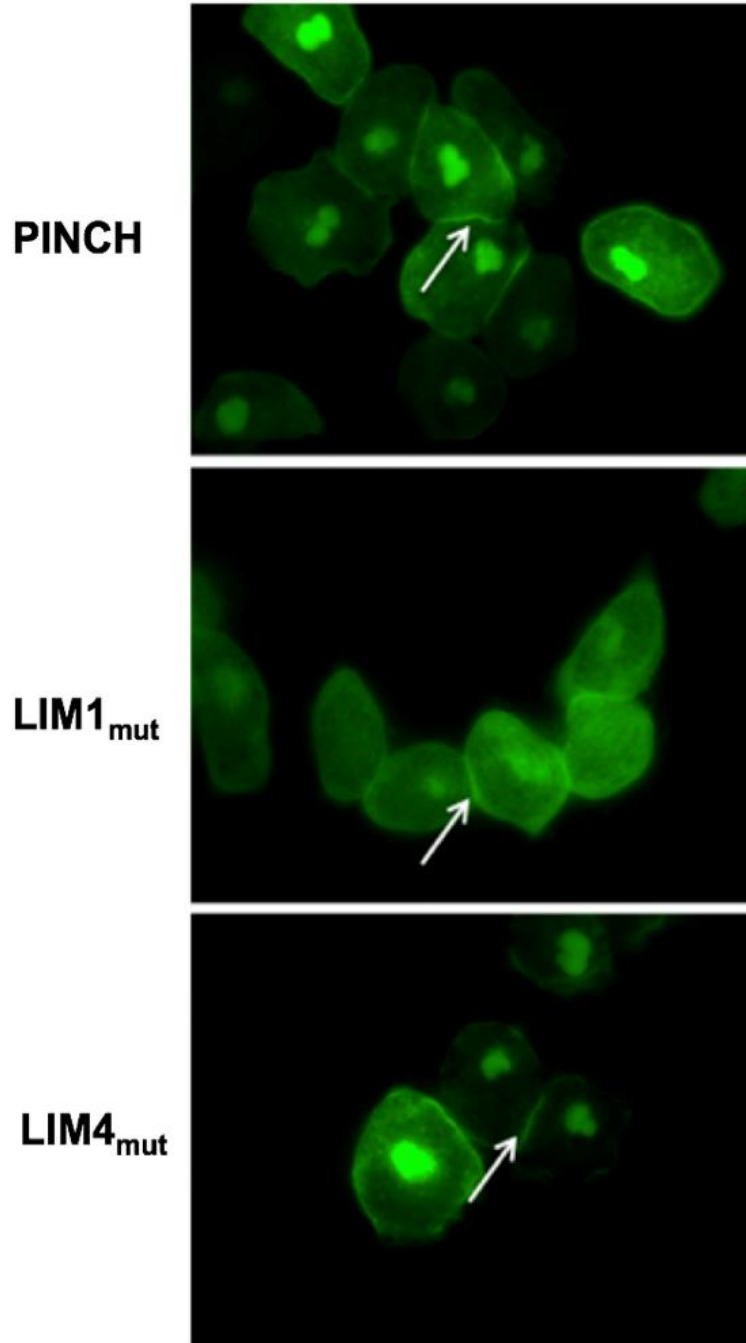


**Figure 22: GFP-tagged PINCH constructs localize to cell-cell contact sites in activin-induced animal cap cells.** GFP-tagged PINCH (A), LIM1<sub>mut</sub> (B), and LIM1<sub>mut</sub> (C) localize to the nucleus and nascent forming cell boundaries between migrating cells. The LIM1 and LIM4 domain do not interfere with PINCH localization to these sites. White arrows indicate the cell-cell contact sites.

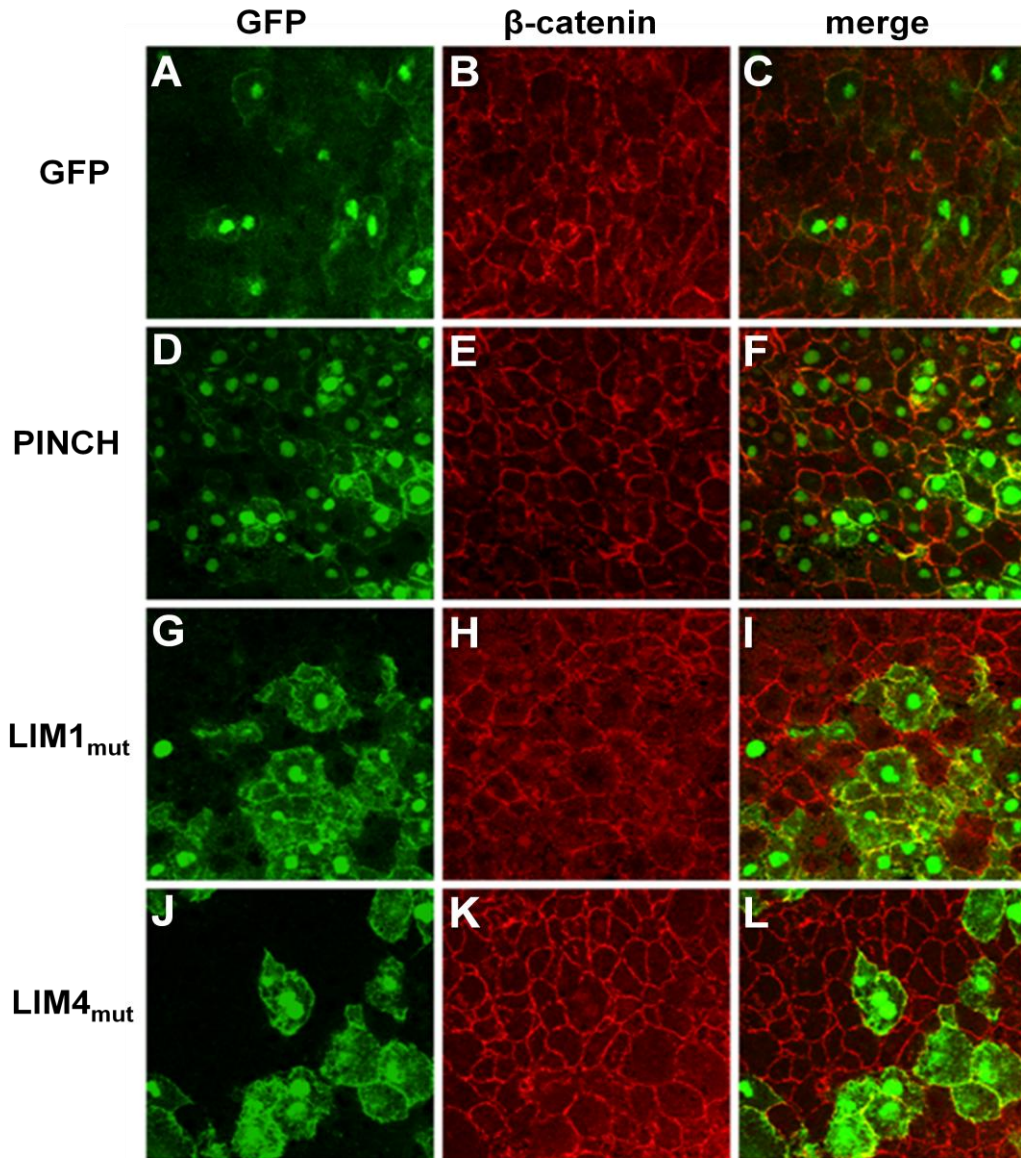


**Figure 23: PINCH localizes to adherens junctions at cell-cell boundaries in the BCR.** Embryos injected with mRNA encoding (A-C) GFP, or GFP-tagged PINCH (D-F), LIM1<sub>mut</sub> (G-I), or LIM4<sub>mut</sub> (J-L) were fixed at stage 11.  $\beta$ -catenin localizes to cell borders in the BCR (B, E, H, K). Embryos injected with mRNA encoding GFP shows the GFP tag does not localize to cell boundaries (A) and does not colocalize with  $\beta$ -catenin (C). GFP-tagged PINCH co-localizes with  $\beta$ -catenin at cell-cell boundaries (compare [A-C] to [D-F]). Similarly, embryos injected with mRNA encoding LIM1<sub>mut</sub> (G-I) and LIM4<sub>mut</sub> (J-L) co-localize with  $\beta$ -catenin at cell-cell boundaries, indicating the LIM1 and LIM4 domain is not required for this localization.

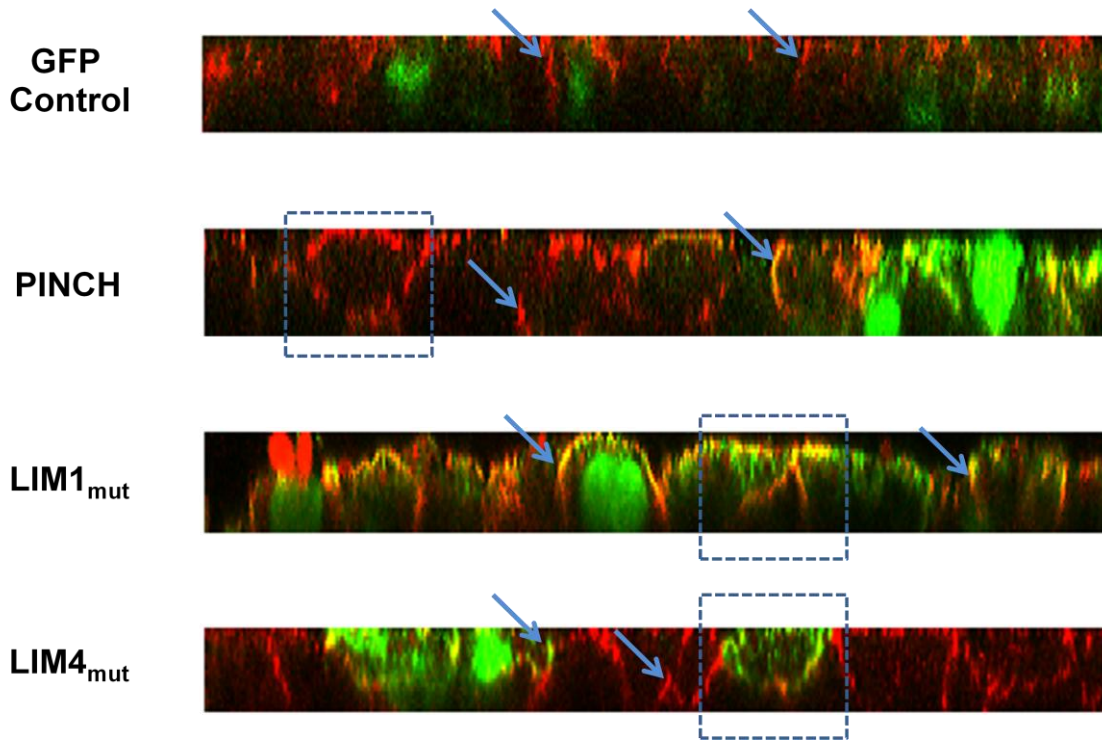


**Figure 24: PINCH colocalizes with  $\beta$ -catenin at cell-cell boundaries in the BCR.** Images represent vertical confocal slices of the BCR from control and PINCH-expressing embryos. GFP expression is represented in green and  $\beta$ -catenin is stained in red.  $\beta$ -catenin normally localizes to the adherens junctions and tissue is organized in the BCR. BCRs from PINCH, LIM1<sub>mut</sub>, and LIM4<sub>mut</sub>-expressing embryos show tissue disorganization characterized by the basally shifted adherens junctions (blue arrows) and an increase layer of cells (dotted boxes).

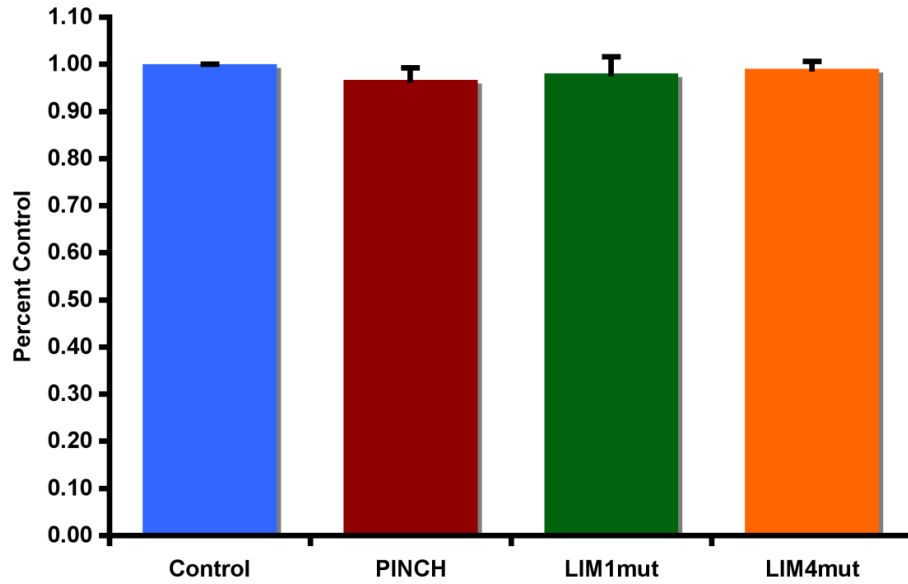


**Figure 25: PINCH does not influence cell adhesion to C-Cadherin.** Cells were plated on the extracellular domain of C-cadherin and counted pre-wash and post-wash to remove non-adherent cells. The values for each construct are presented as a percentage of the control cells that attached. Control, PINCH, LIM1<sub>mut</sub>, and LIM4<sub>mut</sub> expressing cells show similar affinity for cadherin



## Chapter 4. Discussion

### 4.1 Cloning and Characterization of *Xenopus* PINCH

*Xenopus* PINCH was successfully cloned using RT-PCR. The amino acid sequence revealed features common to other known PINCH proteins. These include the five conserved LIM domains and nuclear localization and export signals. Analysis of the amino acid sequence revealed a high degree of similarity with human (98.2%), murine (97.8%), chicken (97.8%) and zebrafish (97.8%) PINCH-1 proteins. These interspecies similarities indicate a highly conserved structure for PINCH suggesting the role played by PINCH may also be conserved across species.

A second cDNA coding for PINCH was found using RT-PCR. As *Xenopus* is tetraploid I would expect to find another closely related cDNA representing a second gene. While there is a 92.5% nucleotide similarity between the two sequences it is not clear that this represents a second allele. There is an additional T residue at position 48 that results in a frame shift downstream disrupting the open reading frame (Fig. A.3). It is not clear if this represents the true sequence or is a result of errors in the RT-PCR procedure. For this reason, the second clone was not investigated further.

Although there are two known PINCH isoforms in mammals (64), it is likely that only a single PINCH isoform exists in *Xenopus*. As expected for two distinct genes that have arisen through duplication, mammalian PINCH-1 shows an approximately 80% similarity to PINCH-2. In contrast, the very high similarity at the nucleotide level between the two clones I isolated suggests that the second clone is unlikely to represent a PINCH-2 ortholog. Furthermore, only a single PINCH EST has been found in both *Xenopus laevis* and *Xenopus tropicalis* (65), and

there does not appear to be a gene encoding PINCH-2 in the *Xenopus tropicalis* genome (66). The lack of a PINCH-2 in *Xenopus* is interesting as PINCH-2 in mammals has been implicated in negatively regulating PINCH-1 binding interactions. The over-expression of PINCH-2 in human embryo kidney cells displaces PINCH-1 from ILK and suppresses integrin-mediated cell spreading and migration (34). These observations suggest that both PINCH proteins compete for the binding site on ILK and have opposing effects on cellular behaviour. However, the presence of only one PINCH homolog in *Xenopus* makes for a simpler model to study the regulation of PINCH in integrin-mediated cell behaviours.

The RT-PCR results indicate that *Xenopus* PINCH mRNA is expressed ubiquitously throughout early embryogenesis. PINCH mRNA is expressed maternally and continues to be expressed zygotically post-MBT. While there does not appear to be a temporal regulation of PINCH expression there is a spatial restriction of mRNA localization. PINCH mRNA is localized to the animal region of the two cell embryo. PINCH is expressed in the BCR at the onset of gastrulation coinciding with both the localized cell movements of epiboly and FN matrix assembly. PINCH continues to be expressed in the marginal zone of the gastrula, particularly in the pre-involution mesoderm where cellular rearrangements of convergent extension are actively driving gastrulation movements. However, PINCH is not present in the post-involution mesoderm that also undergoes convergent extension suggesting PINCH is not essential for convergent extension. This would suggest that PINCH plays a regulatory role in pre-involution mesoderm rather than being a required component of the molecular machinery that drives cell intercalations. Interestingly, PINCH expression is coincident with expression patterns of both the  $\alpha 5\beta 1$  integrin (8, 67) and FN (68) during later stages of development. At the neurula stage, *Xenopus* PINCH is expressed in the cranial neural crest. This expression is

consistent with chicken PINCH which is expressed in both the neural folds and neural crest cells during avian embryogenesis (69). Neural crest cell migration in *Xenopus* has been demonstrated to require  $\alpha 5\beta 1$  and FN (70), suggesting a possible role of PINCH in regulating integrin-ECM interactions during neural crest cell migration. During the tadpole stages, PINCH strongly localizes to the somite boundaries and the pharyngeal pouches, neural folds and heart. Based on the work in this study, PINCH appears to function independent of integrins during gastrulation (discussed below) but the similar expression patterns between PINCH and  $\alpha 5\beta 1$  during post-gastrulation stages suggest an integrin-associated function later in development.

#### **4.2 PINCH is required for *Xenopus* embryogenesis**

In the *Xenopus* embryo, cell intercalation underlies epiboly in the BCR and CE in the marginal zone of the embryo (17). Embryos over-expressing PINCH, LIM1<sub>mut</sub>, and LIM4<sub>mut</sub> have normal mesoderm patterning but fail to undergo the proper morphogenetic movements during gastrulation. In these embryos the thickness of BCR suggests a failure in the cell movements that define epiboly. Compared to control BCRs that are two cell layers thick, PINCH, LIM1<sub>mut</sub> and LIM4<sub>mut</sub>-expressing BCRs consist of at least three to four cell layers suggesting a failure in deep cell intercalative behaviour. Since  $\alpha 5\beta 1$ -FN ligation has been shown to be required for the cell rearrangements driving the thinning of the BCR (46), this failure in cell intercalation may be due to a lack of FN and not a direct result of PINCH mis-expression. However, the cells in the BCR have a loose arrangement and appear to lack strong cell-cell interactions. This is not observed in embryos lacking a FN matrix (46) and indicates that PINCH may play a role in cell-cell interactions (discussed below). While I cannot attribute any defined role for PINCH, over-expression of LIM1<sub>mut</sub> and LIM4<sub>mut</sub> has a weaker effect on blastopore closures than PINCH

alone. This suggests that the LIM1 and LIM4 domains of PINCH are titrating molecules required for driving gastrulation. Future work could directly address this question using co-IPs or yeast two-hybrid assays.

### **4.3 PINCH and Cell Adhesion**

#### **4.3.1 Effect of PINCH on Cell-Matrix Adhesion**

Cells along the BCR use  $\alpha 5\beta 1$  integrin to bind to FN and assemble a matrix at the onset of gastrulation (43). FN matrix is severely inhibited in PINCH, LIM1<sub>mut</sub>, and LIM4<sub>mut</sub>-expressing embryos. Compared to the long, dense, organized fibrils in control embryos, the BCRs from both PINCH and LIM1<sub>mut</sub> embryos display short and sparse fibrils. LIM4<sub>mut</sub>-expressing embryos show a less profound effect and the matrix consists of few long fibrils that are highly disorganized. The presence of sparse fibrils in BCRs expressing PINCH and the LIM1<sub>mut</sub> and LIM4<sub>mut</sub> constructs suggests that  $\alpha 5\beta 1$  can still interact with FN in these embryos. This is supported by my cell adhesion assays where activin-induced animal cap cells expressing PINCH and the LIM1<sub>mut</sub> and LIM4<sub>mut</sub> constructs show no differences in adhesion to FN. The similar distances travelled in these cells also suggest that PINCH expression does not influence cytoskeletal dynamics in migrating cells. These observations indicate that over-expression of PINCH has no effect on the adhesive properties of  $\alpha 5\beta 1$  integrin. Insights into a possible role PINCH plays in regulating FN matrix assembly can be postulated from the appearance of distinctive fibrils in LIM4-expressing BCRs. The FN matrix observed in LIM4<sub>mut</sub>-expressing embryos is similar to BCRs over-expressing tyrosine phosphatase PTP-PESTr (71). The long fibrils in these embryos were suggested to be a result of BCR cells moving with respect to one

another (either by radial intercalation or cell division) and the FN that is bound to  $\alpha 5\beta 1$  may be passively stretched revealing cryptic sites necessary for limited FN polymerization (71). Such a scenario may explain limited FN assembly in my experiments. Such an interpretation is supported by the observation that the LIM4<sub>mut</sub> construct has effects on cell-cell adhesion (discussed below). Despite the disruption of FN assembly by PINCH, LIM1<sub>mut</sub> and LIM4<sub>mut</sub> my results indicate this is not through the direct regulation of integrin interactions with FN

In tissue culture models PINCH regulation of  $\alpha 5\beta 1$  integrin has been intimately tied to the formation of the IPP complex. ILK binds directly to both PINCH and parvin and recruits the heterotrimeric complex to  $\beta 1$  and  $\beta 3$  integrin tail at sites of integrin adhesion (20). My observations indicate that PINCH localizes to focal adhesions in *Xenopus* A6 cells. These observations are consistent with an IPP complex as ILK and parvin were also found at these sites of cell-matrix adhesion (Studholme, unpublished data). Surprisingly, LIM1<sub>mut</sub> localizes to focal adhesions indicating that ILK does not influence PINCH localization to cell-matrix adhesion sites in A6 cells. This raised the question whether the PINCH-ILK complex exists in *Xenopus*. My co-IP analysis shows that ILK is not detected in a pull-down with PINCH, indicating that this interaction is not likely to occur *in vivo*. This finding has been confirmed in embryos where a pull-down with parvin detected ILK but not PINCH (Studholme, unpublished data). There is previous evidence for ILK-independent recruitment of PINCH in invertebrates. *C.elegans* PINCH ortholog UNC-97 is involved in the assembly of integrin cell adhesion complexes in body wall muscle. In the absence of UNC-97, both ILK and integrin fail to organize normally but are capable of co-localizing at the muscle cell membrane (72). This indicates that there is no obligate interaction between PINCH and ILK as has been described in tissue culture (40). A similar scenario occurs in *Drosophila wech* mutants where PINCH

localization is undisturbed despite ILK recruitment being compromised. Furthermore, a *Drosophila* PINCH variant lacking the LIM1 domain has been shown to retain the capacity to localize to cell-matrix adhesion sites (73). An ILK-independent function of PINCH has been further suggested in *Drosophila* where a PINCH<sup>Q38A</sup> mutant completely rescues the PINCH null phenotype despite being unable to associate with ILK (74). Significantly, both *C. elegans* and *Drosophila* do not have a PINCH-2 ortholog. Perhaps the reduced dependence of PINCH localization on ILK in these species reflects an alternative form of regulation. Together, these observations support the data from my work suggesting that PINCH is regulated independently of ILK *in vivo*.

#### **4.3.2 A role for PINCH in Cell-Cell Adhesion**

As gastrulation proceeds BCR cells change shape from round to polygonal indicating an increase in tension across the BCR (75). Over-expression of both LIM1<sub>mut</sub> and LIM4<sub>mut</sub> results in an irregular shape and arrangement of cells in the BCR. Cells over-expressing these mutated constructs are large, round and overlap neighbouring cells indicating reduced tension across the BCR. This suggests that cell-cell adhesion has been compromised. The maturation of adherens junctions has been demonstrated to be an indicator for increased cell-cell adhesion and tension (13). My data indicate that PINCH is actively recruited to nascent cell-cell junctions in dissociated animal cap cells. In the embryo, PINCH localizes strongly to adherens junctions, suggesting that PINCH may play a role in the maturation or stabilization of these cell junctions during the course of development. A role for PINCH in cell junctions has been previously established in *C. elegans* where PINCH homolog UNC-97 is required for the assembly and stability of muscular adherens (46). Such a scenario in the BCR is supported by my observations

where over-expressing PINCH, LIM1<sub>mut</sub> and LIM4<sub>mut</sub> appear to basally shift the typical apical localization of adherens junctions. The disorganized epithelial structure and the overlapping cells in BCRs suggest tissue tension is comprised and are consistent with my previous findings that BCR cells appear to be more loosely arranged in PINCH, LIM1<sub>mut</sub>, and LIM4<sub>mut</sub>-expressing embryos. Together, my data suggests that PINCH may be regulating tension in the BCR, possibly through changes in cell-cell adhesion.

A decrease in tension within the BCR has been demonstrated previously to inhibit the assembly of a FN matrix (13). Because our results demonstrate that PINCH, LIM1<sub>mut</sub>, and LIM4<sub>mut</sub>-expressing embryos show an inhibition of FN matrix assembly independent of integrin function, it is possible that PINCH affects this process through mediating changes in cell-cell cohesion and tension across the BCR. A decrease in cell-cell cohesion and organization might explain why BCR cells are not able to generate the tension need to assemble a matrix despite the presence of FN fibrils. While an increase in C-cadherin adhesion independent of changes in surface expression is required to generate the tension across the BCR (13, 62, 76), the regulation of cell-cell adhesion in embryos over-expressing PINCH is not easily interpreted. PINCH strongly localizes to cell boundaries in the BCR. However, over-expressing PINCH, LIM1<sub>mut</sub>, or LIM4<sub>mut</sub> does not affect the ability of cells to bind to the extracellular domain of C-cadherin. These data suggest that PINCH has no effect on C-cadherin-mediated adhesion in dissociated animal cap cells. However, caution should be used when extrapolating evidence obtained from dissociated cells to the embryo. Recent studies on cadherin-adhesion indicate that experimentally generated differences in C-cadherin adhesion that produce quantifiable results *in vitro* may not be sufficient to drive observable changes during morphogenesis in the *Xenopus* embryo (77). My experiments measuring cadherin adhesion are not refined and may be

providing a generalized outcome. *Ex vivo* experiments such as cell re-aggregations and cell sorting assays will help support or discard the notion that PINCH regulates cadherin mediated-adhesion.

Although PINCH does not appear to regulate cadherin adhesion, evidence gleaned from existing cell signalling pathways suggest an alternate mechanism through which PINCH could possibly regulate cell-cell adhesion. Recent studies examining the Eph-Ephrin pathway indicate this signalling pathway acts in parallel to cadherins in regulating cell-cell adhesion. For instance, over-expression of wild type ephA-2 receptors in human mammary epithelial cells decreased cadherin-mediated cell adhesion without influencing the level of cadherins or the composition of adherens junctions (78). Interestingly, both eph receptors and cadherins signal through similar downstream effector molecules. For instance, PINCH binding partner Grb4 has been shown to bind to phosphorylated ephrin receptors and couple these receptors with downstream effectors of PAK and Rac GTPase. These two effector proteins have previously been shown to function downstream of cadherin adhesion and influence FN matrix assembly (13). These observations raise the possibility that PINCH-Grb4 complex binds to tails of eph receptors at cell-cell junctions and transduces signals that influence cell-cell adhesive behaviour.

#### **4.4. Conclusions**

*Xenopus* PINCH was successfully cloned and determined to be a PINCH-1 ortholog. There is no PINCH-2 in *Xenopus* suggesting a primitive form of regulation. As such, *Xenopus* is a good model to investigate the role of PINCH in regulating cell behaviour. My data indicate that PINCH has multiple roles during *Xenopus* gastrulation, including the assembly of a FN matrix and driving morphogenetic movements such as epiboly. Most interestingly, PINCH regulates



cell adhesion during gastrulation but not through cadherin or integrin receptors. During early development, PINCH functions independent of ILK as mutations in the LIM1 domain has no effect on cell adhesion. This is supported by my data showing that PINCH is unlikely to be part of the IPP complex *in vivo*. Moreover, my data suggests the regulation of cell adhesion appears to be mediated through the LIM4 domain. As such, this raises the possibility that the PINCH-Grb4 interaction plays an active role in mediating cell-cell adhesion through the eph-ephrin pathway.

## Chapter 5. Future Directions

While my work has provided hints as to the role PINCH plays in *Xenopus* development, it is necessary to determine the specific role of PINCH during gastrulation. My work shows over-expressing PINCH in embryos shows an inhibition of FN matrix assembly and defects in cellular movements driving epiboly. A PINCH translation knock-down using morpholinos is necessary to confirm the specific defects seen in these embryos. By eliminating endogenous PINCH expression and rescuing with either wild-type or reintroducing the LIM1 and LIM 4 mutation constructs in the embryo, I will be able to determine domain specific functions.

Both cell adhesion and cell polarity pathways have been proposed to regulate morphogenetic movements during early development. Recent studies show that the eph cell-cell repulsion receptors have crucial roles in tissue separation between pre- and post-involution mesoderm during gastrulation (79). Knockdown studies at the cellular level suggest these receptors play an important role in cell polarizing and migratory activity but not in specification of cell fates (80). PINCH may play a role in this pathway as Grb4 has previously been shown to be recruited to the eph receptor cytoplasmic tails and transduce signals upon ligation to ephrins (81). Alternatively, PINCH expression during gastrulation coincides with members of the cell polarity pathway that are regulated by the P APC and Frizzled receptors (82). xGIT is a protein expressed only in pre-involution tissue but is shown to be suppressed in involuting mesoderm by P APC/xFz signalling. PINCH binding partner Grb4 has been shown to bind to GIT and recruit the complex to ephrin receptors (83), raising the possibility that Grb4 participates in the convergence of both cell polarity and cell adhesion pathways. From the work presented, it is clear that the LIM4 domain is functionally important in regulating cell adhesion. Thus a

direction for future studies is to pursue the Grb4 interaction and determine if PINCH participates in the eph signalling pathway.

## References

- (1) **Dzamba, B.J., Bolton, M.A., DeSimone, D.W.** (2001). The integrin family of cell adhesion molecules. *Cell Adhesion: Frontiers in Molecular Biology*. Oxford, UK: Oxford University Press, 100-154.
- (2) **Takada, D., Ye, X., and Simon, S.** (2007.) The integrins. *Genome Biol* **8**, 215.
- (3) **J Joos, T.O., Whittaker, C.A., Meng, F., DeSimone, D.W., Gnau, V., and Hausen, P.** (1995). Integrin alpha 5 during early development of *Xenopus laevis*. *Mech Dev* **50**, 187-199.
- (4) **Alfandari, D., Whittaker, C.A., DeSimone, D.W., and Darribere, T.** (1995). Integrin aV subunit is expressed on mesodermal cell surfaces during amphibian gastrulation. *Dev Bio.* **170**, 249-261.
- (5) **Joos, T.O., Reintsch, W.E., Brinker, A., Klein, C., and Hausen, P.** (1998). Cloning of the *Xenopus* integrin alpha(v) subunit and analysis of its disruption during early development. *Int J Dev Biol* **42**, 171-179.
- (6) **Hoffstrom, B.G.** (2002) Integrin function during *Xenopus laevis* gastrulation. Diss. University of Virginia, USA, *Dissertations and Thesis*.
- (7) **Hemler, M.E., Kassner, P.D., and Chan, B.M.C.** (1992). Functional roles for integrin alpha subunit cytoplasmic domains. *Cold Spring Harb Symp Quant Biol* **57**, 213-220.
- (8) **Whittaker, C.A. and DeSimone, D.W.** 1993. Integrin alpha subunit mRNAs are differentially expressed in early *Xenopus* embryos. *Development* **117**, 1239-1249
- (9) **Gawantka, V., Ellinger-Ziegelbauer, H., Hausen, P.** (1992) Beta 1-integrin is a maternal protein that is inserted into all newly formed plasma membranes during early *Xenopus* embryogenesis. *Development* **115**, 595-605.
- (10) **Lee, G., Hynes, R. O. and Kirschner, M.** (1984). Temporal and spatial regulation of fibronectin in early *Xenopus* development. *Cell* **36**, 729-740.
- (11) **Mao, Y., and Schwarzbauer, J.E.** (2005a) Fibronectin fibrillogenesis, a cell-mediated matrix assembly process. *Matrix Biol* **24**, 389–399.
- (12) **Pankov, R., Cukierman, E., Katz, B.Z., Matsumoto, K., Lin, D.C., Lin S., Hahn, C., Yamada, K.M.** (2000) Integrin dynamics and matrix assembly: tensin-dependent translocation of alpha(5)beta(1) integrins promotes early fibronectin fibrillogenesis. *J Cell Biol* **148**, 1075–1090.
- (13) **Dzamba, B.J., Jakab, K.R., Marsden, M., Schwartz, M.A., DeSimone, D.W.** (2009). Cadherin adhesion, tissue tension, and noncanonical Wnt signaling regulate fibronectin matrix organization. *Dev Cell* **16**, 421–32.

- (14) **Davidson, L.A., Dzamba, B.J., Keller, R., Desimone, D.W.** (2008). Live imaging of cell protrusive activity, and extracellular matrix assembly and remodeling during morphogenesis in the frog, *Xenopus laevis*. *Dev Dyn* **237**, 2684–2692.
- (15) **Weber, G.F., Bjerke, M.A., and DeSimone, D.W.** (2011). Integrins and cadherins join forces to form adhesive contacts. *J Cell Sci* **124**, 1183-119.
- (16) **Ramos, J.W., and DeSimone, D.W.** (1996). Xenopus embryonic cell adhesion to fibronectin: position-specific activation of RGD-synergy site-dependent migratory behaviour at gastrulation. *J Cell Biol* **134**, 227-240.
- (17) **Keller, R., Davidson, D.A., Shook, D.R.** (2003) How we are shaped: The biomechanics of gastrulation. *Differentiation* **71**: 171-205.
- (18) **Liu, Y., Calderwood, D.A., and Ginsberg, M.H.** (2000). Integrin cytoplasmic domain-binding proteins. *J Cell Sci* **113**, 3563-3571.
- (19) **Burridge, K., and Chrzanowska-Wodnicka, M.** (1996). Focal adhesions, contractility, and signaling. *Annu Rev Cell Dev Bio* **12**, 463-519.
- (20) **Legate, K.R., Montañez, E., Kudlacek, O., and Fässler, R.** (2006). ILK, PINCH and parvin: The tIPP of integrin signalling. *Nat Rev Mol Cell Biol* **7**, 20–31.
- (21) **Hannigan, G.E., C. Leung-Hagesteijn, L. Fitz-Gibbon, M.G. Coppelino, G. Radeva, J. Filmus, J.C. Bell, and S. Dedhar.** (1996). Regulation of cell adhesion and anchorage-dependent growth by a new beta 1-integrin-linked protein kinase. *Nature* **379**, 91–96.
- (22) **Rearden, A.** (2002). A new LIM protein containing an autoepitope homologous to “Senescent Cell Antigen”. *Biochem Biophys Res Commun* **201**, 1124-1131
- (23) **Wang-Rodriguez, J., Dreilinger, A.D., Alsharabi, G.M., Rearden, A.** (2002). The signaling adapter protein PINCH is up-regulated in the stroma of common cancers, notably at invasive edges. *Cancer* **95**, 1387-95
- (24) **Holmqvist, A., Gao, Jingfang., Holmlund, B., Adell, G., Carstensen, J., Langford, D., and Sun, X.** (2012). PINCH is an independent prognostic factor in rectal cancer patients without preoperative radiotherapy – a study in a Swedish rectal cancer trial of preoperative radiotherapy. *Cancer* **12**, 65
- (25) **Zhang, J., Li, Q., and Wang, D.** (2007). Expression of PINCH protein in oral squamous cell carcinoma and its clinicopathological significance. *Chin J Clin Oncol* **20**, 1157-1159
- (26) **Gao, J. Arbman, G., Rearden, A., Sun, X.** (2004). Stromal staining for PINCH is an independent prognostic indicator in colorectal cancer. *Neoplasia*.
- (27) **Gao, J.** (2008). Molecular and biological characteristics of stroma and tumor cells in colorectal cancer. Diss. Linköping University, Sweden, *Dissertations and Thesis*.

- (28) **Rearden, A., Hurford, R., Luu, N., Kieu, E., Sandoval, M., Perez-Liz, G., Del Valle, L., Powell, H., and Langford, T.D.** (2008). Novel expression of PINCH in the central nervous system and its potential as a biomarker for human immunodeficiency virus-associated neurodegeneration. *Neuroscience* **86**, 2535-2542.
- (29) **Fukuda, T., Chen, K., Shi, X., and Wu, C.** (2003). PINCH-1 is an obligate partner of integrin-linked kinase (ILK) functioning in cell shape modulation, motility, and survival. *J Biol Chem* **278**, 51324-51333.
- (30) **Tu, Y., Li, F., Goicoechea, S. and Wu, C.** (1999). The LIM-only protein PINCH directly interacts with integrin-linked kinase and is recruited to integrin-rich sites in spreading cells. *Mol Cell Biol* **19**, 2425–2434.
- (31) **Boulter, E., Grall, D., Cagnol, S., and Van Obberghen-Schilling, E.** (2006). Regulation of cell-matrix adhesion dynamics and Rac-1 by integrin-linked kinase. *FASEB J* **20**, 1489-1491.
- (32) **Tu, Y., Li, F., Wu, C.** (1998). Nck-2, a novel Src homology2/3-containing adaptor protein that interacts with the LIM-only protein PINCH and components of growth factor receptor kinase-signaling pathways. *Mol Biol Cell* **9**, 3367-82.
- (33) **Wu, C., Keightley, S.Y., Leung-Hagesteijn, C., Radeva, G., Coppolino, M., Goicoechea S., McDonald, J.A., Dedhar, S.** (1998). Integrin-linked protein kinase regulates fibronectin matrix assembly, E-cadherin expression, and tumorigenicity. *J Biol Chem* **273**, 528–536.
- (34) **Zhang, Y., Guo, L., Chen, K. and Wu, C.** (2002). A critical role of the PINCH-integrin-linked kinase interaction in the regulation of cell shape change and migration. *J Biol Chem* **277**, 318–326.
- (35) **Veevers-Lowe, J., Ball, S.G, Shuttleworth, A., Kielty, C.M.** (2011). Mesenchymal stem cell migration is regulated by fibronectin through  $\alpha 5 \beta 1$ -integrin-mediated activation of PDGFR- $\beta$  and potentiation of growth factor signals. *J Cell Sci* **124**, 1288–1300.
- (36) **Campana, W.M., Myers, R.R., Rearden, A.** (2003). Identification of PINCH in Schwann cells and DRG neurons: shuttling and signaling after nerve injury. *Glia* **41**, 213–223.
- (37) **Wang, D., Li, Y., Wu, C., Liu, Y.** (2011). PINCH1 Is a transcriptional regulator in podocytes that interacts with WT1 and represses podocalyxin expression. *PLoS ONE* **6**, e17048
- (38) **Li, F., Zhang, Y., and Wu, C.** (1999). Integrin-linked kinase is localized to cell-matrix focal adhesions but not cell-cell adhesion sites and the focal adhesion localization of integrin-linked kinase is regulated by the PINCH-binding ANK repeats. *J Cell Sci* **112**, 4589-4599.

- (39) **Goicoechea, S.M., Tu, Y., Hua, Y., Chen, K., Shen, T.L., Guan, J.L., and Wu, C.** (2002). Nck-2 interacts with focal adhesion kinase and modulates cell motility. *Int J Biochem Cell Biol* **34**, 791-805.
- (40) **Hobert, O., Moerman, D.G., Clark, K.A., Beckerle, M.C., Ruvkun, G.** (1999). A Conserved LIM Protein That Affects Muscular Adherens Junction Integrity and Mechanosensory Function in *Caenorhabditis elegans*. *J Cell Bio* **144**, 45–57.
- (41) **Clark, K.A, McGrail, M and Beckerle, M.C.** (2003). Analysis of PINCH function in *Drosophila* demonstrates its requirement in integrin-dependent cellular processes. *Development* **130**, 2611-21.
- (42) **Keller, R. (2002).** Shaping the vertebrate body plan by polarized embryonic cell movements. *Sci* **298**, 1950-1954.
- (43) **Davidson, L.A., Keller, R., and DeSimone, D.W.** (2004). Assembly and remodelling of the fibrillar fibronectin extracellular matrix during gastrulation and neurulation in *Xenopus laevis*. *Dev Dyn* **231**, 888-895.
- (44) **Ramos, J.W., Whittaker, C.A., and DeSimone, D.W.** (1996). Integrin-dependent adhesive activity is spatially controlled by inductive signals at gastrulation. *Dev* **122**, 2873-2883.
- (45) **Marsden, M., and DeSimone, D.W.** (2003). Integrin-ECM interactions regulate cadherin-dependent cell adhesion and are required for convergent extension in *Xenopus*. *Curr Biol* **13**, 1182-1191.
- (46) **Marsden, M., and DeSimone, D.W.** (2001). Regulation of cell polarity, radial intercalation and epiboly in *Xenopus*: novel roles for integrin and fibronectin. *Dev* **128**, 3635-3647.
- (47) **Lee, G., Hynes, R.O., and Kirschner, M.** (1984). Temporal and spatial regulation of fibronectin in early *Xenopus* development. *Cell* **36**, 729-740.
- (48) **Sive, H.** (1996). *Early Development of Xenopus laevis; Course Manual*. Cold Spring Harbor: Cold Spring Harbor Laboratory Press.
- (49) **Nieuwkoop, P.D. and Faber, J.** (1967). *Normal Table of Xenopus laevis (Daudiri)*. 2nd edition. Amsterdam: North Holland Publishing Co.
- (50) **Chomczynski, P & Sacchi, N.** (1987). Single-step method of RNA isolation by acid guanidinium thiocyanate-phenol-chloroform extraction. *Anal. Biochem.* **162**, 156-9.
- (51) **Sagerström, C. G., Grinblat, Y. and Sive, H. (1996).** Anteroposterior patterning in the zebrafish, *Danio rerio*: an explant assay reveals inductive and suppressive cell interactions. *Development* **122**, 1873-1883.

- (52) **Harland, R.M.** (1991) In situ hybridization: An improved whole-mount method for *Xenopus* embryos. *Methods Cell Biol* **36**, 685–695.
- (53) **Sambrook, D.W., and Russell, J.** (2001). *Molecular Cloning: A Laboratory Manual* (3rd ed.). Cold Spring Harbor Laboratory Press.
- (54) **Spicer, E., Suckert, C., Al-Attar, H., and Marsden, M.** (2010). Integrin  $\alpha 5\beta 1$  is regulated by XGIPC/kermit2 mediated endocytosis during *Xenopus laevis* gastrulation. *PLoS ONE* **5**,
- (55) **DeSimone, D.W., and Johnson, K.E.** (1991). The *Xenopus* embryo as a model system of the study of cell-extracellular matrix interactions. *Methods Cell Biol* **36**, 527-539
- (56) **Winklbauer, R., Müller, H.A.** (2011) Mesoderm layer formation in *Xenopus* and *Drosophila* gastrulation. *Phys Biol* **8**.
- (57) **Chiswell, B. P., Zhang, R., Murphy, J. W., Boggon, T. J., Calderwood D. A.** (2008). The structural basis of integrin-linked kinase-PINCH interactions. *Proc Natl Acad Sci* **105**, 20677-20682.
- (58) **Velyvis, A., Vaynberg, J., Yang, Y., Vinogradova, O., Zhang, Y., Wu, C., Qin, J.** (2003). Structural and functional insights into PINCH LIM4 domain-mediated integrin signaling. *Nat Struct Biol* **10**, 558-564.
- (59) **Ito S., Takahara Y., Hyodo T., Hasegawa H., Asano E., Hamaguchi M., Senga T.** (2010) The roles of two distinct regions of PINCH-1 in the regulation of cell attachment and spreading. *Mol Biol Cell* **21**, 4120-9.
- (60) **Smith, J.C, Price, B.M, Green, J.B, Weigel, D., Herrmann, B.G.** (1991). **Expression of a *Xenopus* homolog of Brachyury (T) is an immediate-early response to mesoderm induction.** *Cell* **67**, 79-87.
- (61) **Longo, D., Peirce, S.M., Skalak, T.C., Davidson, L., Marsden, M., Dzamba, B., and DeSimone D.W.** (2004). Multicellular computer simulation of morphogenesis: blastocoel roof thinning and matrix assembly in *Xenopus laevis*. *Dev Bio* **271**, 210–222.
- (62) **Brieher, W.M, Gumbiner, B.M.** (1994). Regulation of C-cadherin function during activin induced morphogenesis of *Xenopus* animal caps. *J Cell Biol* **126**, 519–527.
- (63) **Chappuis-Flament, S., E. Wong, L.D. Hicks, C.M. Kay, and B.M. Gumbiner.** (2001). Multiple cadherin extracellular repeats mediate homophilic binding and adhesion. *J Cell Biol* **154**, 231–243.
- (64) **Shi, X., Qu, H., Kretzler, M., and Wu, C.** (2008). Roles of PINCH-2 in regulation of glomerular cell shape change and fibronectin matrix deposition. *Am J Physiol Renal Physiol* **295**, F253-263.



- (65) **Bowes, J.B., Snyder, K.A., Segerdell, E., Gibb, R., Jarabek, C.J., Pollet, N., Vize, P.D.** (2009) Xenbase: a *Xenopus* biology and genomics resource. *Nucleic Acids Res.*, doi:10.1093/nar/gkm826
- (66) **Hellsten, U., Harland, R. M., Gilchrist, M. J., Hendrix, D., Jurka, J., Kapitonov, V., Ovcharenko, I., Putnam, N. H., Shu, S., Taher, L. et al.** (2010). The genome of the Western clawed frog *Xenopus tropicalis*. *Science* 328, 633-636.
- (67) **Ransom, D.G, Hens, M.D, DeSimone, D.W.** Integrin expression in early amphibian embryos: cDNA cloning and characterization of *Xenopus* beta 1, beta 2, beta 3, and beta 6 subunits. *Dev Biol.* 1993 Nov;160(1):265-75.
- (68) **DeSimone, D. W., P. A. Norton, and R. O. Hynes. 1992.** Identification and characterization of alternatively spliced fibronectin mRNAs expressed in early *Xenopus* embryos. *Dev. Biol.* 149:357–369.
- (69) **Martinsen, B.J, Neumann, A.N, Frasier, AJ, Baker, C.V.H, Krull, C.E, Lohr, J.L.** (2006). Pinch-1 expression during early avian embryogenesis: Implications for neural crest and heart development. *Dev Dyn* 235, 152–162.
- (70) **Alfandari, D, Cousin, H., Gaultier, A., Smith, K., White, J.M., Darribere, T., and DeSimone, D.W.** (2001) *Xenopus* ADAM 13 is a metalloprotease required for cranial neural crest-cell migration. *Curr Biol* 11, 918–930
- (71) **Cousin, H., and D. Alfandari.** (2004). A PTP-PEST-like protein affects alpha5-beta1-integrin-dependent matrix assembly, cell adhesion, and migration in *Xenopus* gastrula. *Dev Biol* 265, 416–432.
- (72) **Norman K. R., Cordes S., Qadota H., Rahmani P., Moerman D. G.** (2007) UNC-97/PINCH is involved in the assembly of integrin cell adhesion complexes in *Caenorhabditis elegans* body wall muscle. *Dev Biol* 309, 45–55
- (73) **Zervas, C. G., Gregory, S. L. and Brown, N. H.** (2001). *Drosophila* integrin-linked kinase is required at sites of integrin adhesion to link the cytoskeleton to the plasma membrane. *J Cell Biol* 152, 1007-1018.
- (74) **Elias, M.C., Pronovost S.M., Cahill K.J., Beckerle M.C., Kadrmas, J.L.** (2012) A critical role of Ras Suppressor-1 (RSU-1) revealed when PINCH-Integrin-linked Kinase (ILK) binding is disrupted. *J Cell Sci.*
- (75) **Lecuit, T., Lenne, P.F.** (2007) Cell surface mechanics and the control of cell shape, tissue patterns and morphogenesis. *Nat Rev Mol Cell Biol* 8, 633–644
- (76) **Gumbiner, B.M.** (2005) Regulation of cadherin-mediated adhesion in morphogenesis. *Nat Rev Mol Cell Biol* 6, 622-634

- (77) **Ninomiya, H., David, R., Damm, E.W., Fagotto, F., Niessen, C.M., and Winklbauer, R. (2012).** Cadherin-dependent differential cell adhesion in *Xenopus* causes cell sorting in vitro but not in the embryo. *J Cell Sci* 125, 1877-83.
- (78) **Fang, W.B., Ireton, R.C., Zhuang, G., Takahashi, T., Reynolds, A., Chen, J. (2008).** Overexpression of EPHA2 receptor destabilizes adherens junctions via a Rho-A dependent mechanism. *J Cell Sci* 121, 358-368
- (79) **Park, E.C., Cho, G.S., Kim, G.H., Choi, S.C., Han, J.K. (2011).** The involvement of Eph-Ephrin signaling in tissue separation and convergence during *Xenopus* gastrulation movements. *Dev Biol* 350, 441–450.
- (80) **Rørth, P. (2009)** Collective Cell Migration. *Annu Rev Cell Dev Biol* 25, 407–29
- (81) **Cowan, C.A, Henkemeyer, M. 2001.** The SH2/SH3 adaptor Grb4 transduces B-ephrin reverse signals. *Nature* 413, 174–79
- (82) **Köster, I.. (2010)** Transcriptional regulation of tissue separation during gastrulation of *Xenopus laevis*. *Diss. University of Heidelberg, Germany, Dissertations and Thesis.*
- (83) **Segura I.D., Essmann C.L., Weinges S., Acker-Palmer, A. (2007).** Grb4 and GIT1 transduce ephrinB reverse signals modulating spine morphogenesis and synapse formation. *Nat Neurosci* 10, 301 - 310

## Appendix A

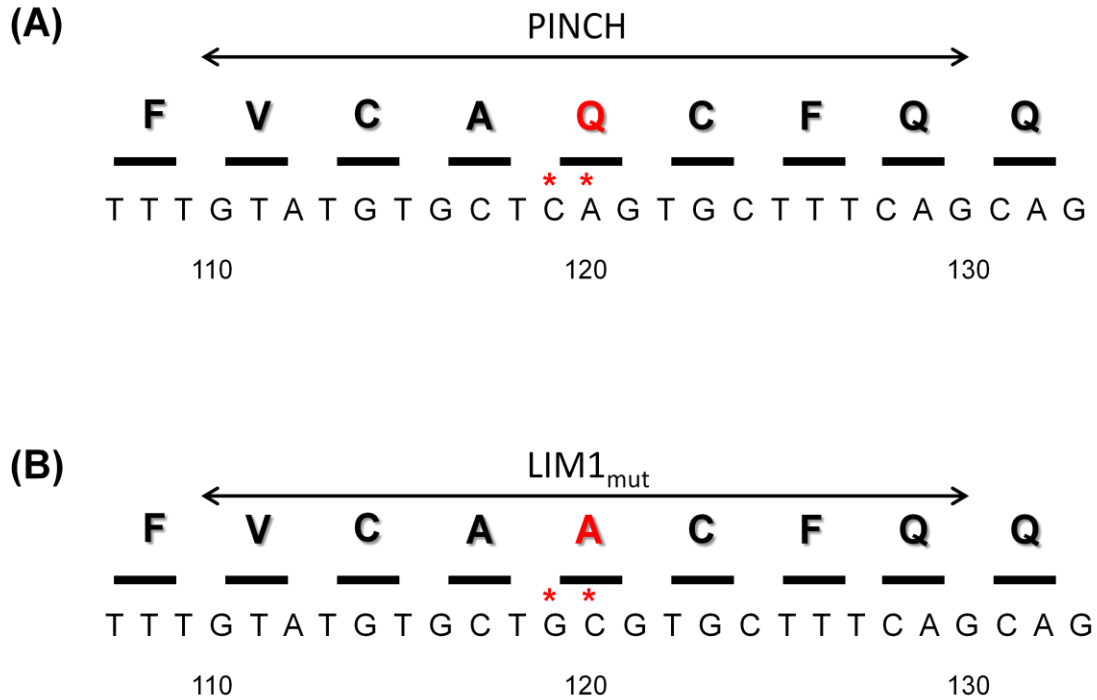


**Figure A.1 Confirmation of PINCH and LIM1<sub>mut</sub> LIM1-domain coding sequences.** To generate the LIM1<sub>mut</sub> coding sequence (B), the coding sequence of PINCH LIM1 domain (A) was mutated at positions 119 (C → G) and 120 (A → C). Nucleotides substitutions are indicated with red astericks. These mutations translate into an amino acid exchange from phenylalanine (Q) to alanine (A) (CAG → GCG).

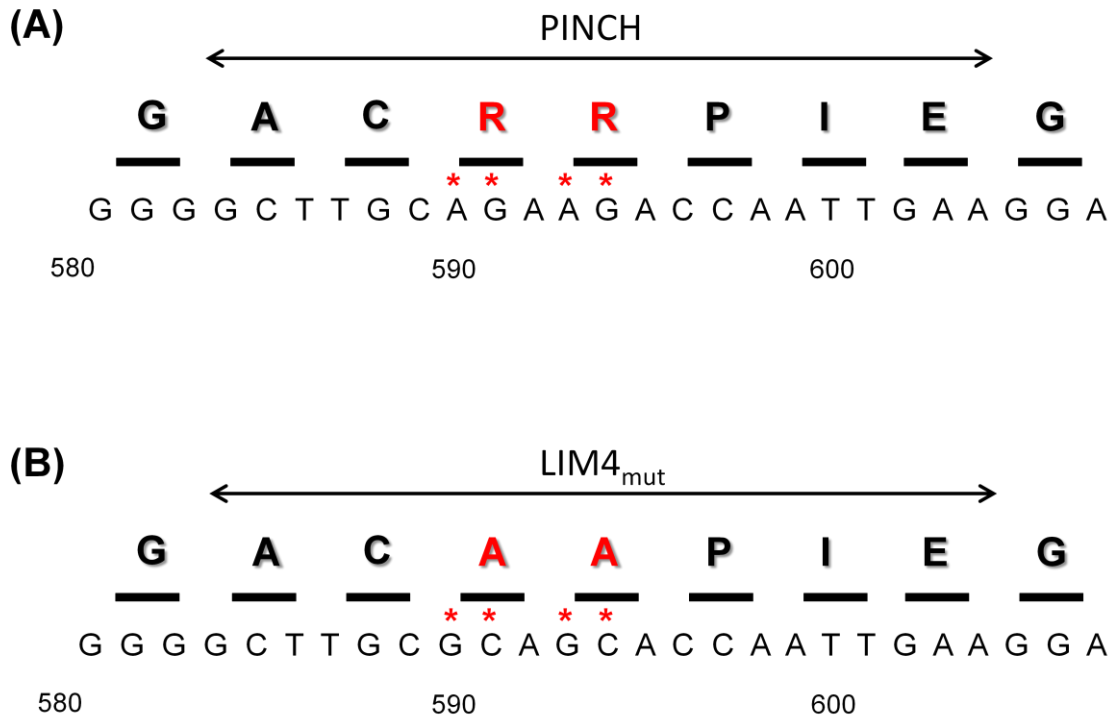


**Figure A.2 Confirmation of PINCH and LIM4<sub>mut</sub> LIM4-domain coding sequences.** To generate the LIM4<sub>mut</sub> coding sequence (B), the coding sequence of PINCH LIM4 domain (A) was mutated at positions 590 (A → G), 591 (G → C), 593 (A → G), and 594 (G → C). Nucleotides substitutions are indicated with red astericks. These mutations translate into an amino acid exchange from two phenylalanine residues (QQ) to alanine residues (AA) (AGAAGA → GCAGCA).

```

PINCH clone 1 ATGGC...AAATGCTCTGGCAAATGCAATTTGTGAGCGCTGTCGATCTGG-1TTTGGCTCCTTC
PINCH clone 2 ATGGC...AAATGCTCTGGCAAATGCAATTTGTGAGCGCTGTCGATCTGG1TTTGGCTCCTTC

PINCH clone 1 TGAAAAGATTGTCAAACAGCAACGGAGAGCTGTACCATGAGCAGTGTGGTGTATGTGCTCA
PINCH clone 2 TGAAAAGATTGTCAAACAGCAACGGAGAGCTGTACCATGAGCAGTGTGGTGTATGTGCTCA

PINCH clone 1 GTGCTTTCAGCAGTTTCAGAGGGACTCTTCTATGAGTTTGAAGGTAGAAAAATATTGTGA
PINCH clone 2 GTGCTTTCAGCAGTTTCAGAGGGACTCTTCTATGAGTTTGAAGGTAGAAAAATATTGTGA

PINCH clone 1 GCATGATTTCCAAATGCTGTTTGTCTCCCTGCTGCCATCAGTGTGGTGAATTTATCATTGG
PINCH clone 2 GCATGATTTCCAAATGCTGTTTGTCTCCCTGCTGCCATCAGTGTGGTGAATTTATCATTGG

PINCH clone 1 CCGTGTCATTAAAGGCTATGAACAACAGCTGGCATCCAGAGTGTTCGGCTGTGATATCTG
PINCH clone 2 CCGTGTCATTAAAGGCTATGAACAACAGCTGGCATCCAGAGTGTTCGGCTGTGATATCTG

PINCH clone 1 TCAGCAAAGTCTGGCAGACATTGGATTTGTTAAGAACGCTGGAAGGCACCTTGGCCCTC
PINCH clone 2 TCAGCAAAGTCTGGCAGACATTGGATTTGTTAAGAACGCTGGAAGGCACCTTGGCCCTC

PINCH clone 1 CTGTCACAACCGAGAGAAAAGCAAAGGACTTGGCAAATATATCTGCCAGAAGTGCCATGC
PINCH clone 2 CTGTCACAACCGAGAGAAAAGCAAAGGACTTGGCAAATATATCTGCCAGAAGTGCCATGC

PINCH clone 1 TATTATTGAAGAGCATCCCTTATATTCAAGAATGACCCATATCACCCAGATCATTTTAA
PINCH clone 2 TATTATTGAAGAGCATCCCTTATATTCAAGAATGACCCATATCACCCAGATCATTTTAA

PINCH clone 1 CTGTGCCAACTGTGAAAAAGAGCTGACCCCGATGCTCGTGTGTTAAAAGGTGAGCTGTA
PINCH clone 2 CTGTGCCAACTGTGAAAAAGAGCTGACCCCGATGCTCGTGTGTTAAAAGGTGAGCTGTA

PINCH clone 1 TTGCTTACCTTGTACGACAAGATGGGTGTGCCTATATGTGGGCTTGCAGAAGACCAAT
PINCH clone 2 TTGCTTACCTTGTACGACAAGATGGGTGTGCCTATATGTGGGCTTGCAGAAGACCAAGT

PINCH clone 1 TGAAGGACGTGTCTGTAATGCTATGGGAAAGCAGTGGCATGTCCAGCATTGTTGATGCGC
PINCH clone 2 TGAAGGACGTGTCTGTAATGCTATGGGAAAGCAGTGGCATGTCCAGCATTGTTGATGCGC

PINCH clone 1 AAAAGTGTAAAAAACCTTTCTTGGCCATCGCCATTATGAGAGGAAGGGGCTGGCTTACTG
PINCH clone 2 AAAAGTGTAAAAAACCTTTCTTGGCCATCGCCATTATGAGAGGAAGGGGCTGGCTTACTG

PINCH clone 1 CGAGACACATTACAACCAGCTTTTGGAGATGCTGCTTTTCATTGCAATCGTGTTATTGA
PINCH clone 2 CGAGACACATTACAACCAGCTTTTGGAGATGCTGCTTTTCATTGCAATCGTGTTATTGA

PINCH clone 1 A- - - - - AAGTTAACACTCAAGAACAATTTGTTGAATTTGACATGAAGCCTGCTCG
PINCH clone 2 AAGTTAACACTCAAGAACAATTTGTTGAATTTGACATGAAGCCTGCTCG

PINCH clone 1 TAAAGAAATGCTATGAGAAAGTTTCTCTGGAGTTAAAGAAAAGGCTTAAAGAAAGCTATCTGA
PINCH clone 2 TAAAGAAATGCTATGAGAAAGTTTCTCTGGAGTTAAAGAAAAGGCTTAAAGAAAGCTATCTGA

PINCH clone 1 ACCACTAGCTAAAAAATAAGTGGGTCTTACTGACACCACAGGGTGAAGACTNGGATAAG
PINCH clone 2 ACCACTAGCTAAAAAATAAGTGGGTCTTACTGACACCACAGGGTGAAGACTNGGATAAG

PINCH clone 1 CATTCTAGAGCGGCCGCC
PINCH clone 2 CATTCTAGAGCGGCCGCC

```

**Figure A.3 PINCH cDNA clone sequences identified using RT-PCR** An additional T residue at position 48 shifts the reading frame of PINCH clone 2. PINCH clone 1 was used in this thesis.

-56

**GG A TC CTC CCC CAA TCT CTG GCT CCC ATG CTG GGC**

**GTT GTG GGG ATG ACG AAC AGC AAC **ATG** GCAAAT**

1

**Figure A.4: Upstream sequence of translational start site in all PINCH clones.** All of the PINCH constructs contain a short region (56bp) upstream of the translational start site. The forward primer (*BamHI*) is highlighted in green. The translational start site is highlighted in red (position 1).